A leading-edge based method for correction of slope-induced errors in ice-sheet heights derived from radar altimetry

Weiran Li [1], Cornelis Slobbe [1], and Stef Lhermitte [1]

[1]Department of Geoscience and Remote Sensing, Delft University of Technology, Delft, The Netherlands

Correspondence: Weiran Li (w.li-7@tudelft.nl)

Abstract. Satellite radar altimetry has been an important tool for cryospheric applications such as measuring ice-sheet height or assessing ~~snow/ice anomalies~~ anomalies in snow and ice properties (e.g., the extensive melt in Greenland in 2012). Although accurate height measurements are key for such applications, slope-induced errors due to undulating topography within the kilometre-wide ~~pulse-limited~~ beam-limited footprint can cause ~~multi-meter~~ multi-metre errors. Therefore different correction methods have been developed ranging from the slope method to the point-based method. Each of these methods have shortcomings as they either neglect the actual topography or the actual footprint that can be estimated by a combination of the leading edge and topography. Therefore, a novel Leading Edge Point-Based (LEPTA) method is presented that corrects for the slope-induced error by including the leading edge information of the radar waveform to determine the impact point. The principle of the method is that only the points on the ground that are within range determined by the ~~begin~~ beginning and end of the leading edge are used to determine the impact point.

Benchmarking of the LEPTA method to the slope- and point-based method based on CryoSat-2 LRM acquisitions over Greenland in 2019 shows that heights obtained by LEPTA outperform the other methods when compared to ~~ICESat-2~~ ICESat-2 observations, both in the flat, interior regions of Greenland and in regions with more complex topography. The median difference between the slope-corrected CryoSat-2 heights using LEPTA and the ICESat-2 heights is ~~almost negligible~~at millimetre level, whereas the ~~other methods can have a 0.22 m and 0.69~~ slope and point-based methods can respectively have a 0.21 m and 0.48 m difference, and the Level-2 data provided by ESA have a ~~0.01~~ 0.01 m difference. The median absolute deviation of height differences between CryoSat-2 and ICESat-2, which we use as an indicator of the variation of errors, is also the lowest ~~in LEPTA (0.09~~ for LEPTA (0.09 m) in comparison to the aforementioned methods (~~0.22 m and 0.13 m~~ 0.19 m for slope method and 0.10 m for point-based method) and ESA Level-2 data (~~0.15~~ 0.14 m). Although ESA Level-2 products and the point-based method have good performance in either median and median absolute deviation, LEPTA stably outperforms the other methods. Based on that, we recommend considering LEPTA ~~to obtain~~ for obtaining accurate height measurements with radar altimetry data, especially ~~in regions with complex topography~~towards the margins of the LRM coverage where the surface slopes increase.

1 Introduction

Satellite radar altimetry is a key tool for assessing the status and dynamics of the cryosphere as it allows constructing digital elevation models (DEMs) (Slater et al., 2018), deriving height change of ice sheets ~~(Helm et al., 2014a)~~(Hurkmans et al., 2012; Helm et al., 20 , understanding seasonal variations of snow (Adodo et al., 2018), and estimating snowpack properties (Lacroix et al., 2008). To obtain accurate information on heights, altimetry processing involves correction for instrument errors, atmospheric effects, tidal effects, and slope-induced errors ~~(Bouzinac, 2012). Among the correction processes, correction~~ (Helm et al., 2014a; Hai et al., 2021) . Of crucial importance is the correction for slope-induced errors ~~has been of crucial importance~~ as they can affect the ~~results of~~ obtained height measurements significantly. For example, according to the error propagation in Brenner et al. (1983), the CryoSat-2 satellite at an altitude of ~~730~~ 730 km, and measuring heights of a terrain with a 0.6° slope, can give a vertical offset of approximately ~~40~~ 40 m and a horizontal offset of ~~7.6~~ 7.6 km.

To correct for the slope-induced errors, different methods have been developed (Brenner et al., 1983; Remy et al., 1989; Bamber, 1994; Roemer et al., 2007). The most widely used methods involve both a correction to the height as well as a relocation of the satellite measurement location from nadir to the expected impact point on the terrain. These correction methods are typically referred to as ~~'~~‘slope’ and ~~'~~‘point-based’ methods (Levinsen et al., 2016). The slope method assumes constant surface slope parameters within the beam-limited altimeter footprint and calculates the relocated ~~longitude, latitude~~ latitude, longitude, and height according to trigonometry (Brenner et al., 1983; Remy et al., 1989; Bamber, 1994). The point-based method ~~takes the full height information within the~~ uses a topographic model within the beam-limited satellite footprint and searches for ~~the smallest range from the satellite to the terrain surface~~ minimum range between the satellite and a surface area in the size of the pulse-limited footprint (Roemer et al., 2007).

Although both methods have been refined and applied with reliable results, they both show methodological shortcomings. The slope method, for example, tends to ignore the local topography within the footprint and therefore may not be accurate enough in undulating areas (Levinsen et al., 2016). The point-based method of Roemer et al. (2007), on the other hand, is more accurate in the undulating regions (Roemer et al., 2007; Levinsen et al., 2016) as it considers the detailed topography, but by assuming a fixed footprint size, it neglects the actual footprint that illuminates the terrain. For example, by taking the averaged range within the assumed footprint, this method may ignore part of the terrain that actually contributes to the return signal, or assumes that part of the terrain not visible to the satellite could contribute to the return signal (See Fig. 1). The recent availability of high-resolution DEM products ~~, however,~~ provides the opportunity to determine the part of the terrain contributing to the rise of the leading edge, and therefore ~~helps determining~~ can determine the actual footprint of the radar altimeter.

To overcome the shortcomings of both methods, we present a novel Leading Edge Point-Based (LEPTA) method (Section 3) that exploits ~~high resolution~~ high-resolution DEM information to correct for the slope-induced error by including the leading edge information of the radar waveform to determine the impact point. The principle of the method is that only the points on the ground that are actually within ~~range~~ the range interval determined by the begin and end of the leading edge are used to ~~determine~~ compute the impact point.

The paper is organised as follows. The Section 2 describes the data used for radar altimetric processing and result assessment are described. Thenassessment of the results. In Section 3, the different methods used for correction and the the correction of the slope-induced errors as well as the assessment workflow are introduced. The results and analysis/discussion will then be presented.

2 Data and pre-processing

To assess the performance of the LEPTA method, we apply it to all CryoSat-2 LRM acquisitions over Greenland in 2019 and benchmark it to the slope- slope and point-based methods by comparing it with laser altimeter ICESat-2 data. height measurements. In Sections 4 and 5 we present, analyse, and discuss the results. Finally, we conclude by emphasising the main findings.

2 Data and pre-processing

2.1 CryoSat-2 observations

On the interior of the Greenland ice sheet, data acquired by CryoSat-2 are in Low Resolution Mode (LRM). LRM is the conventional pulse-limited mode that requires correction for slope-induced errors. The pulse-limited LRM footprint is approximately 1.65 km in diameter, and the footprint of this mode is approximately 1.65 beam-limited footprint is approximately 14.39 km in diameter (Bouzinac, 2012)(Hai et al., 2021). Our evaluation employs all acquisitions data acquired from Jan. -Dec. 1 to Dec. 31, 2019, resulting in approximately 2.4×10^6 valid acquisitions, in order to ensure abundant spatial and temporal coverage2.2×10^6 measurements. In particular, we use level-1b (L1b) Baseline D data (Meloni et al., 2020).

To process the waveform information and obtain height estimations, Level-1b (the L1b) (European Space Agency, 2019a) waveforms were retracked using the offset centre of gravity (OCOG) method (Wingham et al., 1986) documented in Bamber (1994), . We used OCOG because of its precision and robustness (Bamber, 1994; Schröder et al., 2019). According to Davis (1997), a 10% threshold is ideal for detecting ice-sheet height change (or strong volume scattering (Aublanc et al., 2018)), a 20% threshold is the most proper for estimating the absolute or true ice-sheet height, and a 50% threshold is the most appropriate for estimating the absolute height when the waveform is dominated by surface scattering e. g. Antarctic ice shelves. A 10% threshold is also applied when volume scattering is strong (Aublanc et al., 2018). (Davis, 1997; Aublanc et al., 2018). In this study, we follow the recommendation of Davis (1997) and use a 20% threshold is selected to obtain accurate absolute height estimations of the interior of the Greenland ice sheet, as to obtain estimates of the true ice-sheet elevation. This allows a comparison with ICESat-2 data. Aublanc et al. (2018), who used 25%, highlighted that this choice is a compromise between surface scattering pure surface scattering (in which case the threshold should be around 50%) and volume scattering (Aublanc et al., 2018). The 20%threshold is close to the (10%). In the first case, one would underestimate the true elevation, and in the other overestimate it. Hence, as pointed out by Davis (1997), '*the 20% retracking point provides a reasonable estimate of the true ice-sheet elevation in only an average sense*'. An additional note is that ESA used a 25% threshold use by ESA in the L2 processing (Bamber, 1994). This is also a more realistic threshold when the performance is assessed with ICESat-2, which measures the snow-air surface. In addition, in this process, waveforms that do not have a distinguishable noise and beginning of leading edge are droppedWaveforms are removed in case they meet one of the following empirically derived criteria: i) the integrated normalised power exceeds 150, ii) the normalised power in the first 10 range bins is larger than 0.2, or iii) no peaks are identified in the waveform.

Additionally, Level-2I To benchmark our results, level-2I (L2I) height data obtained with the OCOG retracker from European Space Agency (2019b) were usedas benchmark dataset. In the L2I products the slope-induced error is corrected with the Helm et al. (2014b) DEM, of which the resolution is 1 km ×1 km (Helm et al., 2014a). which has a resolution of 1×1 km (Helm et al., 2014a). To enable a fair comparison with our in-house processed L2 data, all L2I height measurements are removed for which the waveforms meet one of the criteria mentioned above.

2.2 ArcticDEM

Within the slope correction methods, a reference DEM is required to determine the impact point. The slope method therefore uses a low resolution DEM (or a downsampled version) To compute a correction for the slope-induced errors, a DEM is needed. Here, the slope method uses a low-resolution DEM as it assumes a constant slope within the radar pulse-limited footprint. On the contrary, the point-based methods (i.e., LEPTA and the point-based method proposed by (Roemer et al., 2007) Roemer et al. (2007)) require DEMs with higher resolution, to provide the full information of the local terrain.

In this study, ArcticDEM was used as reference DEM as it is constructed from recent stereo satellite imagery and is available in high resolution (2 m×2 m2×2 m) (Porter et al., 2018). The systematic error of ArcticDEM is less than 5 5 m (Noh and Howat, 2015) and the DEM has been updated since 2016. ArcticDEM was downsampled to 900 m resolution is low-pass filtered to 2 km resolution by applying a block-mean filter for the slope-based method and to 100 100 m resolution for the point-based and LEPTA methodsused as a compromise between computational efficiency and the demand for high resolution. We also downsample it to various resolutions (200 m to 900 m with a 100 m interval) to . The use of 100 m resolution instead of 2 m is a compromise to computational efficiency. To assess the impact of DEM resolution affects on the correction methods (Subsection Section 3.3), we vary the resolutions from 100 m (200 m for the slope method, for computational efficiency) to 900 m with a 100 m interval, and from 1 to 8 km with a 1 km interval.

2.3 ICESat-2 observations

For validation of the different slope correction methods, the ICESat-2 L3A Land Ice Height products (Smith et al., 2020a) were usedas they provide independent accurate processed height measurements(ATL06) product (Smith et al., 2020a) is used. ICESat-2 uses the Advanced Topographic Laser Altimeter System (ATLAS) which emits green light pulses and counts the received photons (Abdalati et al., 2010). The laser beams are configured in a 2×3 array. The distance between and within beam pairs is ∼3.3 km and ∼90 ~ 3.3 km and ~ 90 m, respectively (Smith et al., 2019). The along-track resolution of the land ice height products is ∼20 product is ~ 20 m (Smith et al., 2020b). The ATL06 products have a known geolocation accuracy/bias of less than 10 m (https://nsidc.org/sites/nsidc.org/files/technical-references/ICESat2_ATL06_Known_Issues_ v005.pdf, last access: December, 2021). A comparison between ICESat-2 data are available at the National Snow and Ice Data Center (NSIDC)website (). and ArcticDEM is shown in Appendix A. The results show that the median ICESat-2 height for the different beam pairs is up to 0.02 m higher than ArcticDEM. The median absolute deviation of the differences is 0.81 m for all beam pairs.

3 Methods

3.1 Slope correction methods

The geometry of different slope-induced error correction methods is briefly are conceptually illustrated in Fig.1. 1. The impact points estimated from the slope method, the point-based method, and LEPTA are represented by P_s, P_p and P_l. The 'low-resolution DEM' (2 km) is only used by the slope method, whereas the point-based method and LEPTA use a 'high-resolution DEM' (100 m). The slope method computes a correction based on the surface slopes obtained from a DEM, whereas the point-based method and LEPTA are based on the range between the satellite and the terrain. Illustration of

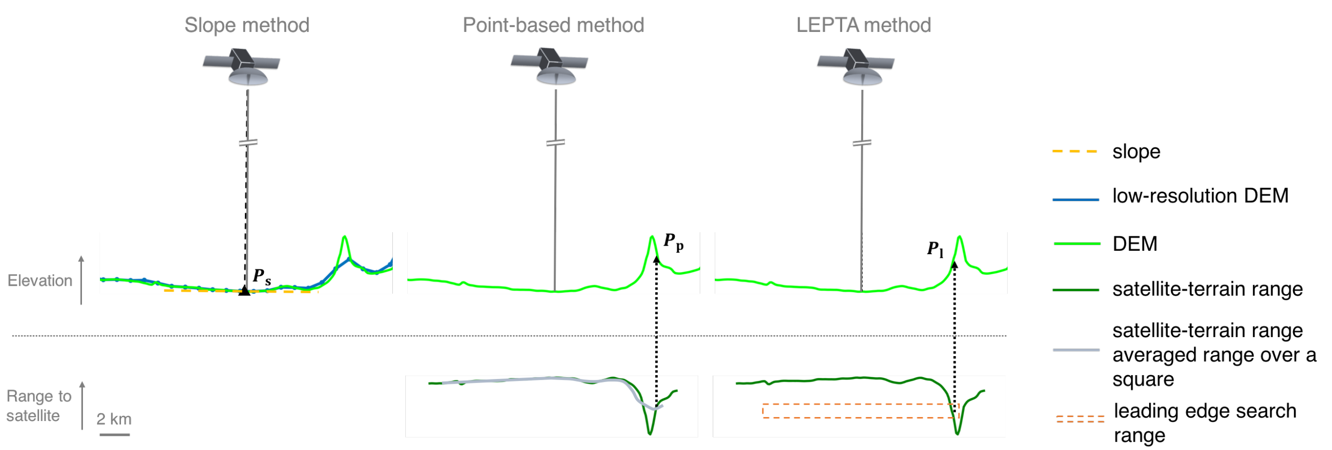

Figure 1. Illustration Conceptual illustration of different slope-induced error correction methods. The impact points estimated from the slope method, the point-based method, and LEPTA are represented by P_s, P_p and P_l. The slope method applies computes a surface slope correction based on the surface slopes obtained from a DEM, and whereas the point-based method and LEPTA apply are based on the satellite-terrain range , as represented by dark green curvesbetween the satellite and the terrain.

difference in horizontal geometry of point-based (left) and LEPTA (right) methods. The star marks the nadir point of the satellite measurement, as well as the centre of the region. The brown polygons indicate the assumed CryoSat-2 footprint. The coloured points at the centre of the polygons (denoted as P_p and P_l) are the computed CryoSat-2 impact points, and the coloured points are ICESat-2 measurements. The black line indicates the distance between the corrected CryoSat-2 measurement and the nearest neighbour in ICESat-2 measurements.

3.1.1 Slope-based Slope correction method

The slope method uses the slope of the low resolution low-resolution DEM at the nadir point to compute the impact point. As such it It assumes that the slope within the CryoSat-2 pulse-limited footprint is constant, and is defined by direction θ and magnitude Φ (Cooper, 1989; Bamber, 1994). The corrected height, represented by In our implementation, θ and Φ are computed in the same map projection and grid as ArcticDEM. The gridded θ and Φ are then interpolated to the satellite nadir point. The corrected height (h_C, is), corresponding to the height of the impact point P_s, can then be obtained by (Bamber, 1994):

$$h_C = R_I \frac{R_s \sin(\Phi - \Gamma)}{\sin\Phi} - R_\alpha = R_s sin(\Phi - \Gamma)/sin\Phi - R_\alpha, \tag{1}$$

where Γ is the central angle between the satellite and P_s

$$\Gamma = \sin^{-1}\left(\frac{R\sin\Phi}{R_s}\right), \tag{2}$$

$$R_s = R_\alpha + h_S, \tag{3}$$

$$R_\alpha = \frac{\rho\nu}{\nu\cos^2\theta + \rho\sin^2\theta}, \tag{4}$$

$$\nu = \frac{a}{\sqrt{1 - e^2\sin^2\phi}}, \tag{5}$$

$$\rho = \frac{a(1 - e^2)}{\sqrt{(1 - e^2\sin^2\phi)^3}}, \tag{6}$$

R represents the retracked range, R_I is the rangebetween P_s and the centre of the curvature at P_s, and R_s is the range between the centre of the curvature and the satelliteat latitude and longitude λ. R_α represents the radius of Earth's curvature at P_s a and e the semi-major axis and eccentricity of the reference ellipsoid being used, and ϕ is the latitude of the satellite. The corrected location of the impact point in latitude ϕ_C and longitude λ_C (in radians) are computed as

$$\phi_C = \frac{\pi}{2} - 2sin - 2\sin^{-1}\left(\frac{X + \Delta x}{2R_\alpha cos\lambda_C}\right)\left(\frac{X + \Delta x}{2R_\alpha\cos\lambda_C}\right), \tag{7}$$

$$\lambda_C = tan\tan^{-1}(\left(\frac{Y + \Delta y}{X + \Delta x}\right)), \tag{8}$$

where X and Y define the position of ~~P_s~~ the satellite in Cartesian coordinates~~and~~

$$\Delta x = R_\alpha \Gamma cos\theta$$

,

$$\Delta x = R_\alpha \Gamma \cos\theta, \tag{9}$$

and

$$\Delta y = R_\alpha \Gamma \sin\theta. \tag{10}$$

$$\Delta y = R_\alpha \Gamma sin\theta$$

Application of the slope-method in Fig. 1 shows that the impact point will be assumed at the position P_s. Inaccuracies usually occur when this method is applied to complex terrains, due to the simplification of the complex topography to a constant slope Levinsen et al. (2016).

3.1.2 Point-based correction method

The point-based method directly uses the topographic information from the ~~a-priori~~ a priori DEM to find the impact point (P_p). It does so by minimising the mean distance $\bar{R}_P$ to the satellite over a pre-defined fixed-size rectangular footprint area (e.g., ~~2 km ×2 km in Roemer et al. (2007)~~1.65 × 1.65 km in Hai et al. (2021)). Assuming the pre-defined rectangular footprint ~~(~~with area A ~~)~~ consists of n DEM grid cells, $\bar{R}_P$ is computed by (Roemer et al., 2007):

$$\bar{R}_P = \frac{1}{R}\sum_{j=1}^{n} A_{Pj}\bar{R}_{Pj},$$

$$\bar{R}_P = \frac{1}{A}\sum_{j=1}^{n} A_{Pj}\bar{R}_{Pj}, \tag{11}$$

where A_{Pj} and $\bar{R}_{Pj}$ are the area ~~and range of~~ of and range to each grid cell j. The ~~position (defined by ϕ_c and λ_c) of the footprint that minimises~~ point for which $\bar{R}_P$ is ~~then obtained~~ minimal is referred to as P_p with latitude ϕ_c and longitude λ_c. The range between the satellite and P_p is referred to as r_p. ~~The~~ In line with Roemer et al. (2007), we use the 100 m DEM to find an approximate position. The final point is obtained by a second search in the vicinity of the approximate position for which we use an up-sampled DEM of 10 × 10 m. The corrected height h_C is computed as (Roemer et al., 2007)

$$h_C = h_N + r_p - (h_S - h_I), \tag{12}$$

where h_N is the surface height of the nadir point relative to the reference ellipsoid (i.e., the ellipsoidal height of the satellite h_S minus the retracked range ~~), h_S is the ellipsoidal height of the satellite,~~ R), and h_I is the DEM height of P_p. ~~It~~ Eq. (11) also shows, however, that this approach can take DEM points into account that actually do not contribute to the rise of the leading edge (i.e., points that fall outside the pulse-limited footprint).

3.1.3 Leading Edge Point-Based (LEPTA) correction method

The LEPTA method is similar to the point-based method as it also uses the topographic information from the a-priori a priori DEM to find the impact point (P_l), but differs in the search method of the impact point. Instead of pre-defining a fixed rectangular pulse-limited footprint size, the LEPTA-method LEPTA method identifies the parts of the terrain within the beam-limited satellite footprint that contribute to the rise of the leading edge. To identify these parts, we define the beginning of the leading edge as the point where the normalised waveform power (values are between 0 and points, we use a beam-limited satellite footprint of 14.39×14.39 km (Hai et al., 2021) centred around the nadir point and a search range bounded by r_{begin} and r_{end}:

$$r_{\text{begin}} = \max(r_{1\%}, r_{20\%} - \Delta r), \tag{13}$$

$$r_{\text{end}} = \min(r_{90\%}, r_{20\%} + \Delta r), \tag{14}$$

where $r_{1\%}$ and $r_{90\%}$ refer to the retracked ranges obtained using, respectively, a 1) is greater than 0.05. The end of the leading edge is more difficult to define as there might be multiple peaks before the waveform reaches its maximum power. Here, we defined it as the point that is located at a distance % and 90% threshold retracker (Davis, 1997), $r_{20\%}$ is the OCOG retracked range using a 20% threshold to obtain the snow-air interface (see Section 2.1), and Δr is a user-defined threshold. Δr from the range obtained by applying the OCOG retracker mentioned in Subsection 2.1. In this study, we used Δr =3.5 m . The robustness of the results regarding the choice of Δr will be further assessed in Subsection 4.3.

For each point, the distances are computed between the satellite and all DEM grid points within an area of 8×8 km centred around the nadir point. Thereafter, the DEM points are identified for which the range is within the interval defined by the beginning and end of the leading edge. is used to avoid the search range ($r_{\text{end}} - r_{\text{begin}}$) becomes unrealistically large. For all experiments, we use a value of 1.25 m based on an empirical optimisation of Δ_r (see Section 4.3). In case no DEM grid points are identified , the interval is adjusted by the minimum within the search range, we add the difference between the computed distances and the retracked range . Next, the range to the closest DEM point and r_{begin} to r_{begin} and r_{end}.

The location of P_l is computed as the average of all K identified DEM grid points. Finally, the corrected height h_C is computed by

$$h_C = h_N + \frac{1}{K}\sum_{i=1}^{K}(r^i_{\text{DEM}} - (h_S - h^i_{\text{DEM}})), \tag{15}$$

where h^i_{DEM} and is the ellipsoidal height of the ith identified DEM grid point and r^i_{DEM} are the height of and the range between the satellite and the ith identified DEM grid point$i$. . By using averaging to compute P_l, it is theoretically possible that the average location is outside the actual pulse-limited footprint (e.g. when the impact points form a donut shape or two equally large but disjoint sets of points). These occurrences can be easily identified.

One of the advantages of the LEPTA method compared to the point-based method is that it includes points that contribute to the rise of the leading edge signal but are outside the fixed ~~footprint.~~

~~The difference in footprint and impact points between LEPTA-method and point-based method is illustrated in an example in Fig. ??. The brown areas indicate the areas on the surface that (is assumed to)~~ (square) pulse-limited footprint, and rejects points that do not contribute to the ~~return signal for both the~~ rise of the leading edge signal but are inside the pre-defined pulse-limited footprint. An additional advantage of LEPTA is that it does not apply the recursive computation process as the point-based ~~and LEPTA method. Contrary to the point-based~~ method, ~~for LEPTA this area may take any shape. This example is an illustration of the theoretical advantage of LEPTA~~therefore it speeds up the processing. Assessment of the performance of different methods will be described in ~~Subsection~~ Section 3.2.

3.2 Performance assessment

To assess the performance of the LEPTA method, we benchmark the different methods by comparing their accuracy relative to reference data. First, we directly compare the corrected ~~height measurements~~ heights (h_C) for each method with the reference height from the ~~100~~ 100 m ArcticDEM. Doing so provides a conceptual assessment of the performance of the methods. To compare ~~the corrected heights (h_C)~~ with the DEM, we ~~bilinearly~~ bi-linearly interpolate the DEM heights to the CryoSat-2 locations (~~h_{DEM}~~h_{DEMC}). Then, the CryoSat-2 measurements are grouped in ~~50 km × 50 km~~ 50 × 50 km tiles. For each tile, we compute the median and median absolute deviation of the ~~$h_C - h_{\mathrm{DEM}}$ values.~~ $h_C - h_{\mathrm{DEMC}}$ values. This assessment cannot be considered as a validation as ArcticDEM is not an independent dataset. However, it is insightful especially when the CryoSat-2 points do not have a nearby ICESat-2 point.

Second, we compare the corrected height measurements for each method with the ICESat-2 heights. This comparison is done per month, i.e., we compare the CryoSat-2 heights acquired in a particular month to the ICESat-2 heights acquired in the same month. ~~Also here, we group the datasets in tiles of 50 km × 50 km.~~ For each point, we first identify all ICESat-2 points within ~~50~~ 50 m of the CryoSat-2 point. In case ICESat-2 points are available in each quadrant surrounding the CryoSat-2 point, the ICESat-2 heights are interpolated to the CryoSat-2 point using a natural-neighbour interpolation (h_{ICE2}). Otherwise a nearest neighbour interpolation is applied. A natural neighbour interpolation provides a smoother solution (Bobach, 2009) yet requires weighting functions based on the surrounding points. ~~The~~ To correct for the height difference between the locations of the CryoSat-2 and ICESat-2 points over a potential sloping terrain, we apply a correction computed as the height difference between the 100 m ArcticDEM evaluated at the CryoSat-2 (h_{DEMC}) and ICESat-2 (h_{DEMI}) locations. Hence, the differences between the CryoSat-2 and ICESat-2 heights ~~are referred to as~~ (Δh~~. Similar as before~~) become

$$\Delta h = h_C - h_{\mathrm{ICE2}} - (h_{\mathrm{DEMC}} - h_{\mathrm{DEMI}}) \qquad (16)$$

Similar to the comparison with ArcticDEM, we compute for each 50 × 50 km tile the median and median absolute deviation of Δh.

When benchmarking the methods, two aspects of accuracy are assessed. First, we determine the difference between the slope-corrected CryoSat-2 measurements and the reference heights (~~h_{DEM}~~ h_{DEMC} or h_{ICE2}) by means of standard statistical parameters (median, median absolute deviation, mean, and standard deviation). Second, we assess the ~~spatial differences between the~~ variability of the statistics for the different methods. The statistical parameters are computed with and without ~~removing outliers.~~ outliers. Cumulative functions are provided mainly to visualise the percentiles that indicate the distribution of the results and determine the outliers. Here, we consider ~~any difference between h_C and $h_{\mathrm{DEM}}/h_{\mathrm{ICE2}}$ outside the 10th and 90th percentiles~~ $h_C - h_{\mathrm{DEM}}$ or Δh outside the 10–90th percentile range as an outlier. Probability distribution functions are provided to visualise the overall distribution of results. The skewness parameter is provided as long tails of the probability distribution are not completely visualised. In addition, tiles including less than 10 measurements are rejected for visualisation and interpretation, as the statistics of these tiles do not represent sufficient data and cannot be informative.

3.3 Sensitivity analysis

The LEPTA method is potentially sensitive to i) the ~~way the ‘end’ of the leading edge is defined (which in turn determines the satellite footprint)~~definition of r_{end} and r_{begin} and hence Δr (see Eqs. (13)–(14)), ii) a potential bias in the DEM, and iii) the resolution of the ~~used~~ DEM. Another aspect that may impact the ~~results~~ height estimates of all methods is the adopted OCOG threshold (see Section 2.1). To assess how our choices impact the results, we ~~conducted~~ conduct a number of sensitivity analyses in which we:

- ~~Varied~~ Vary Δr ~~from 2–5~~ (Eqs. (13) and (14)) from 0.5 to 5 m in steps of ~~0.5 m~~ 0.5 m to define an optimal choice.
- ~~Added~~ Vary the adopted OCOG threshold to determine R and hence h_N (Eq. (16)) from 10% to 90% in steps of 20%, using an optimal choice of Δr for LEPTA.
- Add a bias to the DEM of ~~-7.5–2.5~~ −7.5–2.5 m in steps of ~~2.5 m~~2.5 m, using a 20% OCOG threshold and an optimal choice of Δr for LEPTA.
- ~~Varied~~ Vary the DEM resolution from ~~200–900~~ 200 to 900 m in steps of ~~100 m.~~
- ~~Changed the OCOG threshold from~~ 100 m, and from 1 to 8 km in steps of 1 km, using a 20% ~~to 50%~~OCOG threshold and an optimal choice of Δr for LEPTA.

4 Results

4.1 Comparison with ArcticDEM

~~Benchmarking the different methods to the 100 m ArcticDEM (~~The cumulative distribution of $h_C - h_{\mathrm{DEMC}}$ for all methods (Fig. 2a) shows that most values are within the [-1.0, 3.0] m interval (as shown by 10th and 90th percentiles), although outliers have an ~~important~~ impact on the ~~performance of all methods with multi-metre outliers for the 1st, 5th, 95th and 99th percentiles. We see moreover that the ESA L2I and slope method resultsinclude larger outliers than the point-based and LEPTA methods. Since these outliers have a large~~ interpretation of the results. These outliers have most impact on the ~~mean and standard~~

deviation , we repeated our analysis with all values outside the 10–90th percentile interval removedoverall standard deviation and skewness of $h_C - h_{\text{DEMC}}$, as shown in Table 1 and Fig. 3. Although the distribution curves show a positive bias, the skewness is negative for all methods, showing more or larger negative outliers, as also shown in Fig. B1. Comparison of the methods, however, shows that LEPTA is least affected by such negative outliers.

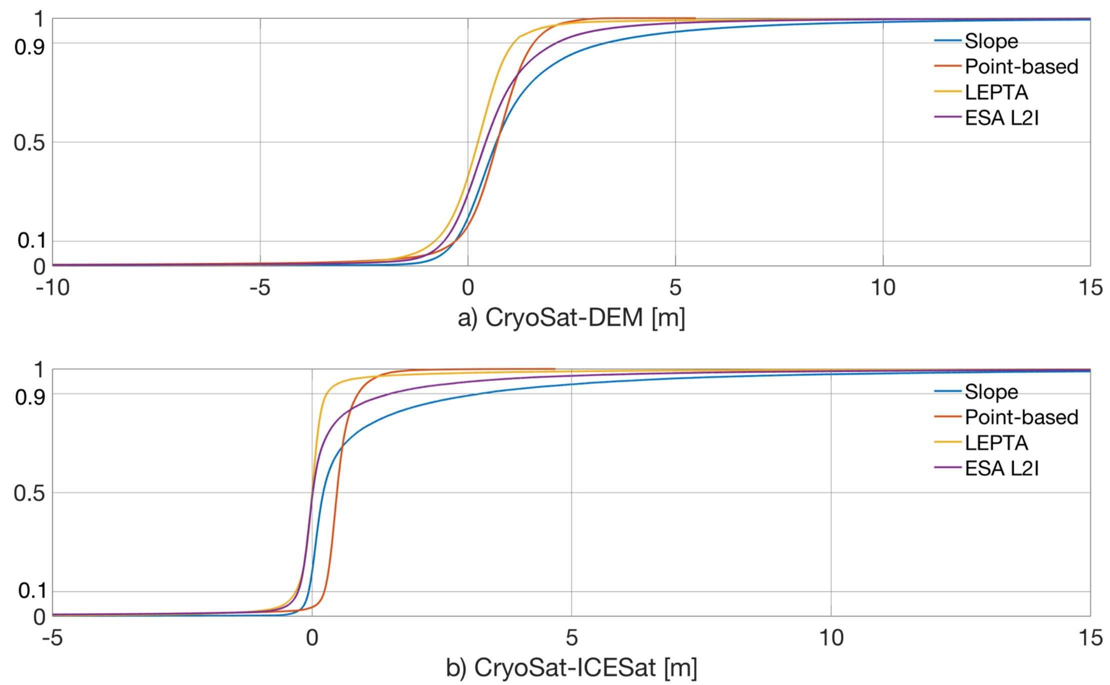

Figure 2. Cumulative distribution figures of a) the difference between CryoSat-2 and ArcticDEM ($h_C - h_{\text{DEM}}$) and b) the difference between CryoSat-2 and ICESat-2 (Δh), including outliers. 10th and 90th percentiles are shown in the figures for outlier removal. For visualisation, x-axis is restricted to [-10, 15] m for figure a and to [-5, 15] m for figure b.

Removing the outliers significantly reduces the standard deviation of $h_C - h_{\text{DEM}}$ $h_C - h_{\text{DEMC}}$ and skewness for all methods and brings the mean closer to the median. Comparison of the mean and median values (Table 1) and probability distribution (Fig.3) indicates moreover 3a) moreover indicates that LEPTA performs best better than other methods when compared with ArcticDEM, with both mean and median differences in height of 0.27 a mean height difference of 0.22 m and a median difference of 0.24 m. The slope method gives results in the largest mean difference of 1.08 0.87 m, while the point-based method gives the largest median of 0.95 0.71 m. The standard deviation (0.44 0.46 m) and median absolute deviation (0.33 m) of 0.34 m) from LEPTA are also the smallest, same as those obtained from the point-based method. The largest $h_C - h_{\text{DEMC}}$ deviation values after outlier removal are given by the slope method, with the standard deviation being 1.09 0.82 m and median absolute deviation being 0.50 m. This shows that the $h_C - h_{\text{DEM}}$ results from the slope method are the least represented by the mean and median, thus are the least ideal. 0.50 m. An additional note is that the mean and median from all methods

~~become above 0, which means~~ are positive, which implies that the heights obtained by these methods are generally higher than ArcticDEM heights. ~~It is also noticed that the ESA L2I products result in more valid outputs than the self-implemented methods.~~

Comparison of the spatial patterns of median and median absolute deviation (Fig. 3) shows large spatial differences in both pattern and magnitude ~~between~~ among the different methods. In general, the largest median and median absolute deviation values occur ~~closer to~~ near the margins of ~~Greenland~~the LRM coverage, where the terrain is steeper. For ~~ESA L2I,~~ the point-based method and LEPTA, the median values on the western side are generally lower than on the eastern side~~of the ice sheet are generally the highest. The median absolute deviation values from ESA~~. For ESA L2I ~~are largest on the western sideof the ice sheet. For~~ products and the slope method, the largest median ~~and median absolute deviation~~ values occur on both eastern and western sides of Greenland, and those from the slope method largely exceed those of the ESA L2I products, the point-based method, and LEPTA. In ~~addition, although hard to distinguish from the plots, 54.2% of~~ general, the ~~grid-cells from the point-based methodhave higher~~ median absolute deviation values of all methods are higher on the western side of the ice sheet than in the interior. For the ESA L2I products and the slope method, the median absolute deviation ~~than LEPTA. High~~ values are also high on the eastern side. These median absolute deviation values ~~from the~~ show that topography affects the different performances of the methods, and the point-based method ~~exist, but are not so concentrated~~ and LEPTA are less affected on the eastern side. In addition, for the point-based method, removing the outliers results in most missing data close to Jakobshavn~~as the other methods~~. Combining the statistics in Table 1 and the spatial distribution of median and median absolute deviation in Fig. 3, it can be concluded that LEPTA ~~has the most ideal performance,~~ performs best when compared with ArcticDEM.

Using averaging in Eq. (15) to compute P_l results in 5.2% of the impact points that are outside the actual footprint. Removing these points as 'unreliable data' (not shown) minimally affects the median and mean (0.26 m and 0.25 m), but improves the median absolute deviation (0.32 m) and standard deviation (0.40 m).

4.2 Validation with ICESat-2 observations

Comparison of CryoSat-2 and ICESat-2 heights (Fig. ~~4~~2b) shows again the ~~importance~~ impact of outliers on the ~~slope-correction methods~~ results, although the outliers are ~~typically~~ generally lower than for the ArcticDEM comparison. ~~For all methods, the Δh values within the visualised range in the probability distribution plot have a longer tail on the right side than the left side of the median. Very large outliers(1st and 99th percentiles) occur at -39.7 m for ESA~~ ESA L2I ~~and at 22.72 m for~~ products, the point-based method and LEPTA have more impacts from negative outliers, while the slope method results in more positive outliers.

With the outliers removed, the standard deviation of Δh values from all methods is greatly reduced, especially for the ESA L2I and slope-method which show the largest outliers ~~.~~ (Fig. 2b). The lowest median (~~0.00~~ 0.00 m), mean (~~0.01~~ 0.00 m), median absolute deviation (~~0.09~~ 0.09 m) and standard deviation (~~0.14~~ 0.13 m) of Δh are obtained by LEPTA, showing that the LEPTA method again outperforms the other methods. The largest median (~~0.69 m) and mean (0.74 m) are~~ 0.48 m) is obtained by the point-based method, and the largest mean (0.51 m), median absolute deviation (~~0.22~~ 0.19 m) and standard deviation

(1.03 0.70 m) are from the slope method. This indicates that the heights obtained by LEPTA are the closest to the ICESat-2 heights.

Comparison The comparison of the height differences between CryoSat-2 and ArcticDEM and vs. ArcticDEM and CryoSat-2 vs. ICESat-2, respectively, shows moreover that the height differences with ICESat-2 are smaller, probably due to the better quality of ICESat-2 data compared to ArcticDEM and the longer time gap between CryoSat-2 and ArcticDEM, as satellite imagery data for generating ArcticDEM were gathered since 2007 (Noh and Howat, 2017; Howat et al., 2019) and co-registered to ICESat from before 2009, whereas ICESat-2 measurements were obtained in the same month as CryoSat-2 data. The comparison between CryoSat-2 and ICESat-2 also results in less data points, as not all CryoSat-2 measurements have corresponding nearby ICESat-2 measurements within the 50 m criterion.

The spatial distribution of the mean median and median absolute deviation of Δh relative to ICESat-2 (Fig. 4) shows clear spatial patternsfor Δh, where the LEPTA methodagain outperforms the other methods with lower height differences compared to the . For the ESA L2I products, the slope method, and the point-based method (i.e. median values of 0 versus 0.69 m, respectively)and more spatially homogeneous patterns compared to ESA 's method, the median differences with respect to the overall median difference are generally negative (positive) in the central part (margins of the LRM zone). For LEPTA, the variability of negative or positive differences is smaller (especially vs. ESA L2I products and the slope method. The latter show for example large errors over the steeper areas near the edges. To sum up, the point-based method generally has the highest median values, while), but with a slightly reversed pattern. This reversed pattern can be explained by LEPTA's definition of r_{begin} and r_{end} that may result in an asymmetry around $r_{20\%}$ that can spatially vary. Figure 4 also shows that LEPTA has the lowest spatial variability of the median absolute deviation, whereas the slope method has shows the largest contrast between the interior and the margins of the LRM zone.

4.3 Sensitivity to the definition of the end of the leading edgesearch range

As mentioned in Subsection Section 3.3, the performance of the LEPTA method relies on the definition of the beginning and end of the leading edge, where the definition of the end of the leading edge is particularly difficultr_{begin} and r_{end} and hence Δr. To assess the sensitivity of LEPTA by to the choice of Δr, we repeated repeat the performance assessment by defining the end of the leading edge as the point which is 2–5 m away from the retracking pointvarying Δr, as introduced in Section 3.3. The results of this Δr sensitivity assessment are summarised in Fig. 5. It shows that , while Δr changes at metre level, the median and the median absolute deviation values of Δh change at millimetre level, and the median absolute deviation values change at centimetre level. This analysis confirms that the method is very only change at centimetre level. More specifically, the median and median absolute deviation increase with increasing Δr. From Fig. 5 we can also conclude that $\Delta r = 1.25$ results in a near-zero median difference compared to ICESat-2. Hence $\Delta r = 1.25$ is used for all experiments.

However, it is not sufficient to conclude that LEPTA is robust to the choice of Δr by merely assessing Δh. The reason is that different Δrs might result in different horizontal locations, which are then compared to potentially different ICESat-2 measurements. Therefore, Fig. 6 shows the differences in the ellipsoidal height and horizontal position of the impact points obtained using $\Delta r = 2$ m (Δr_2) and $\Delta r = 1$ m (Δr_1). This comparison shows whether a Δr change of 1 m can result in large horizontal and vertical offsets. In the interior of the ice sheet this effect is small as the vertical and horizontal offsets resulting from Δr_2 vs. Δr_1 are close to 0. In the margin regions of LRM coverage, however, increasing Δ_r results in lower elevation impact points and horizontal offsets with mean values up to 20 m and standard deviations up to 250 m.

4.4 Assessment of OCOG retracker threshold dependence

The comparison of different slope-correction methods with the ESA L2I products highlights the importance of the OCOG retracker threshold in obtaining R (hence h_N) in the different height estimations. Changing the OCOG retracker threshold from 10% to 90% results in retracked points further away from the satellite and hence lower height estimates (Fig. 7). For all methods, this behaviour is apparent, as the median of Δh is reduced by approximately 1.2 m when the threshold increases from 10% to 90%. Changing the OCOG retracker threshold in LEPTA results only in a change of the height of P_l and does not affect the selection of the DEM points that contribute to P_l. This means that increasing the OCOG retracker threshold actually corresponds to increasing the depth of the radar return within the snowpack or firn. Moreover, Fig. 7 highlights that the adopted OCOG retracker threshold of 20% for LEPTA results in a near-zero median difference compared to ICESat-2, indicating that on average it effectively detects the absolute ice sheet height (Section 2.1). ~~An additional observation is that the slope of the curve of median values decreases with increasing Δr. A reason for this could be that when the range interval is large enough, 1m of increase does not necessarily increase the amount of the illuminated points on the terrain.~~

4.5 Sensitivity to potential biases in the DEM

To assess the sensitivity of the methods to ~~biases in the DEM (e.g. due to surface mass balance changes), we performed the analysis introduced in Subsection 3.3 with ICESat-2 as validation data. Figure~~potential constant ice sheet elevation changes, we perform a sensitivity analysis in which we add biases to the DEM. Figure 8 shows that the slope and the point-based methods are not affected by ~~biases in the DEM , while for LEPTA~~these DEM biases, while it does affect LEPTA. The impact, though, depends on the sign of the bias. Adding a bias between −7.5 and −2.5 m (which corresponds to ice sheet lowering) only changes the ~~median changes about 10 cm when the bias in the DEM is 2.5 m. The~~ median Δh by approximately 2.3 cm, while adding a bias of 2.5 m (which corresponds to an increase in ice sheet elevation) results in a median Δh that is 8.8 cm higher. A similar observation holds for the median absolute deviation ~~is also around 3 cm higher. This is understandable as the presence of a bias in the DEM does not affect the slope or the relative differences between the DEM points, which are the key information to the slope method and the point-based method respectively. However, in the case of LEPTA, when the DEM heights are biased~~of Δh. This dependency on the sign of the bias can be easily understood. The impact point is typically in the area where the range between the satellite and the terrain is smallest. Lowering the DEM and thereby increasing the range to the satellite hence results in a reduced number of DEM grid points within the search range ($r_{\text{end}} - r_{\text{begin}}$). In case no points are found, the search range is ~~different from using the heights of the original DEM heights. Using the same search rangemay ignore some points on the terrain that actually contribute to the waveform leading edge, resulting in a slightly larger bias . This result indicates that LEPTA is relatively sensitive to the bias in DEM heights, compared to other methods~~adjusted (Section 3.1.3). Applying a positive bias, on the other hand, will result in other parts of the terrain being within the search range.

Despite LEPTA's sensitivity to a potential bias in the DEM, however, the median and median absolute deviation of Δh remain lower than the other methods for negative biases up to -7.5 m. In case of a positive bias of 2.5 m, the median absolute deviation of Δh from LEPTA is approximately 8 mm higher than that from the point-based method. In Appendix C, we present the results of a similar analysis as shown in Fig. 6. It shows that the impact of a potential bias in the DEM is largest at the western side of the LRM zone, resulting in vertical and horizontal offsets with mean values up to 2 m and 50 m and standard deviations up to 3.5 m and 700 m, respectively.

4.6 Sensitivity to the resolution of the DEM

Figure 9 shows the effect of changing the DEM resolution on the median and median absolute deviation ~~. The~~ of Δh for different slope correction methods. For both the slope and the point-based method~~has the largest deviation when the DEM resolutionchanges from 200 m to 900 m. Although not directly visible in the plots~~, the smallest median Δh is obtained at 2 km resolution. For the slope method, the median ~~of the slope method changes from 0.29 m to 0.22 m , and that of LEPTA changes from 0.00 m to 0.04 m. The median absolute deviation of LEPTA changes from 0.09 m to 0.10 m. The sensitivity analysis of the DEM resolution again shows the robustness of LEPTAmethod, as well as the importance of accurate high-resolution DEM information for the~~ Δh increases from 0.21 to 0.30 m when the DEM resolution increases from 2 to 8 km. For the point-based ~~method. This is reversed for the slope method where coarser DEM resolutions result in better performance as the overall slope is better represented. This simple assessment confirms that for the~~ method, the variation of median Δh for DEM resolutions between 100 m and 2 km is within millimetre level. Lowering the resolution down to 8 km increases the median to 0.62 m. For LEPTA, the variation of the median Δh for DEM resolutions between 100 m and 1 km is within millimetre level. For lower resolutions, the median Δh increases to 0.23 m (8 km resolution). The smallest median absolute deviation for the slope method (0.19 m) and the point-based ~~method and LEPTA, the height difference from ICESat-2 is small when corrected with a high-resolution DEM, and those from the slope method are small when corrected with a low-resolution DEM.~~

4.7 ~~Assessment of retracker dependence~~

~~Statistics of the height difference between slope-corrected CryoSat-2 measurements and ICESat-2, with 20% and 50% threshold for the applied OCOG retracker. Height statistics are in unit of metres. Outliers are removed using 10th and 90th percentiles. S, P, and L represent the slope method, point-based method, and LEPTA, respectively. S P L S P L median 0.22 0.69 0.00 -0.11 0.30 -0.33 median absolute deviation 0.21 0.13 0.09 0.21 0.14 0.14 mean 0.67 0.74 0.01 0.18 0.27 -0.38 standard deviation 1.03 0.21 0.14 0.76 0.25 0.24 Comparison of the different slope-correction methods with the ESA L2I products highlights the importance of the retracker in the different height estimations. Changing the OCOG threshold from 20% to 50% results in retracked points located further away from the satellite, lowering the height estimations () . For all methods, this expected behaviour is apparent, as the median of the height difference between CryoSat-2 and ICESat-2 reduces with 30 cm and 40 cm compared to the original threshold. The~~ method (0.09 m) are obtained at 2 km resolution. For LEPTA, the smallest median absolute deviation is obtained when using a 1 km resolution, though the values between resolutions of 100 m and 2 km vary at millimetre-level. For resolutions lower than 2 km, the median absolute deviation ~~increases, showing that the height estimations~~

~~from the 50% retracker are slightly more off. This result indicates that the height estimations from LEPTA are dependent on the choice of retracker, which is the same as the other methods~~for both the point-based method and LEPTA increases by approximately 10 cm. For the slope method, the increase is 6 cm.

5 Discussion

~~The combination of~~ The comparison with ArcticDEM and validation based on ~~ArcticDEM and~~ ICESat-2 ~~shows~~ show that the presented LEPTA method outperforms the slope and point-based methods as well as the ESA L2I product in accuracy with lower median, mean, and median absolute deviations~~from the reference datasets. Also in terms of spatial patterns, the LEPTA method outperforms the other methods, especially~~ . Especially in the margin regions of the LRM zone, heights derived from LEPTA correspond more closely to ICESat-2 height measurements, compared to the slope ~~based method that shows large error in the steeper margin regions~~method being used by ESA. This indicates that including leading edge information to determine the impact point ~~has~~ results in an important improvement ~~on~~ of the accuracy of CryoSat-2 LRM height estimations. ~~Our results show moreover that the method is not very sensitive to changes in the definition of the end of the leading edge as it shows only millimetre-level uncertainties for the corrected heights when including multi-metre uncertainties on the definition of the end of the leading edge. However, the definition of the leading edge should be adjusted accordingly when a bias is introduced in the DEM, for example as a result long term height changes due surface mass balance changes since the DEM construction. The DEM resolution also has little impact on the method, although a high-resolution DEM is recommended. On the contrary, the choice of the retracker affects all the methods to a similar extent. This analysis also agrees with the study of Brenner et al. (2007) that the difference between radar and laser altimeters is retracker-dependent.~~

By showing the importance of accurately determining the impact points over steeper margin areas, our results confirm earlier work of Levinsen et al. (2016) in the margin regions, where they also showed that the point-based method outperforms the slope ~~based methods~~method in median absolute deviation values. The improved performance of the point-based method and LEPTA ~~methods~~ method can be explained by the assumption of a constant slope within the footprint in the slope-based method, which results in a biased impact point further away from the satellite than the optimal location (Levinsen et al., 2016). An explanation for ~~this~~ the improved performance of LEPTA over the point-based method can be found in the design of the method which only takes into account areas that ~~are within the footprint~~ contribute to the rise of CryoSat-2 LRM waveform leading edge (Fig. ~~1 and Fig. ??~~ 1).

~~Comparison of the ESA L2 products with the slope-based correction method shows finally~~

Our results also show that the ESA ~~product outperforms standard~~ L2I product outperforms our self-implemented slope correction method. This agrees with Levinsen et al. (2016) who attributed the different performance between the ESA~~L2 products and the~~ 's Envisat Radar Altimetry-2 products and their self-implementation of the slope correction method to the Doppler slope correction step implemented in ESA ~~L2~~ L2I products (Blarel and Legresy, 2012) and ~~DEM differences. The ESA L2 products also provides more valid outputs, compared to the self-implemented~~ differences in the used DEM. We must admit that at this stage an explanation for the difference we obtained is lacking. Detailed analysis (not shown in this paper) shows that the differences cannot be explained by the fact that in our study we use another DEM as well as a different OCOG retracker threshold.

The first sensitivity analysis shows that in terms of bulk statistics, LEPTA is quite robust for the definition of the search range. Compared to ICESat-2, the change in the median is < 1 dm for the interval over which we changed Δr, while the change in the median absolute deviation is at millimetre level. Regionally, the impact may be more significant. In particular, we observe significant changes in the vertical and horizontal position of the impact points towards the margins of the LRM zone. Detailed analysis, not shown, shows that in these areas the mean and standard deviation of the leading edge width are larger. This, in turn, suggests using a larger Δr locally. The use of a spatially varying Δr is hence considered as a potential further improvement of the method.

Increasing the OCOG retracker threshold lowers the height estimates for all methods. ~~This could also be attributed to the Doppler slope correction as it has the advantage of being valid directly for all continental surfaces (Blarel and Legresy, 2012). On the contrary, the self-implemented methods dropped the waveforms that are not similar to the standardised waveform (as in Fig. 1 of Simonsen and Sørensen (2017)). LEPTA also leaves out the points that do not have valid DEM values within the search range. More invalid points are therefore dropped in this process. This phenomenon leaves LEPTA potential for improvement~~For both LEPTA as well as the point-based method, the horizontal position of the impact points does not change. This means that increasing the OCOG retracker threshold actually corresponds to increasing the depth of the radar return within the snowpack or firn. That is, the adopted threshold controls the observed penetration. Our results confirm that using a 20% threshold gives on average comparable height estimates as ICESat-2. It is meanwhile worth noting that the probable scattering of ICESat-2 photons within the snowpack cannot be neglected (https://nsidc.org/sites/nsidc.org/files/technical-references/ICESat2_ATL06_ATBD_r005.pdf, last access: December 2021).

Differently from the slope and point-based methods, LEPTA shows sensitivity to a bias in the DEM. The presence of a bias in the DEM does not affect the slope or the relative differences between the DEM points, which are key to the slope method and the point-based method respectively. However, in the case of LEPTA, when the DEM heights are biased and the search range determined by the waveform leading edge is unchanged, the DEM points used to calculate the impact point of LEPTA are changed. According to Appendix C, this bias mainly affects the margins of the LRM coverage. Overall these bias effects indicate that it is key to have up-to-date, time-varying DEMs when applying LEPTA to correct for slope-induced errors. Changes in the elevation over time will affect the applied correction as well as the location of the impact point. However, in case of non-homogeneous elevation changes (which will result in slope changes) this also holds for the other methods.

Sensitivity to DEM resolution shows that the slope and point-based method perform best with an intermediate DEM resolution (2 km), which is consistent with Levinsen et al. (2016). However, differently from Levinsen et al. (2016) who obtained stable performance for the point-based method between 2 and 4 km DEM resolution, our results show that the performance of the point-based method is stable when the DEM resolution is finer than 2 km. This can be attributed to differences in i) the study area, ii) the used altimeter data, iii) the used DEM to compute the corrections, and iv) the reference data and methods for validation. In principle, the point-based method should perform better with a finer DEM resolution because it has the advantage of using full topography rather than assuming a constant slope, as used by the slope method. While Levinsen et al. (2016)

attributed the optimal 2 km resolution of other methods to the radar altimetry's ability to resolve small-scale surface features, our results show that Δr used by LEPTA to define the pulse-limited footprint may have a different impact (e.g. asymmetry around $r_{20\%}$). Therefore, for future studies, fine-tuning the impact of Δr is still of high importance.

Finally, our experiment focuses on the performance of LEPTA in the CryoSat-2 LRM-covered regions over the Greenland ice sheet, therefore it remains to be studied how it performs over more complex terrains and Antarctica. Since the topography and DEM quality in other regions of the Earth are different from those in Greenland, we expect LEPTA to perform differently, and the impact of Δr can also vary. This phenomenon provides more aspects for future works.

6 Conclusions

Reducing slope-induced errors is a key correction algorithm when ~~applying the radar altimeter data~~ processing LRM data over ice sheets. To correct for this error, different methods have been developed to determine the impact point, which all rely on footprint assumptions: e.g. slope-method, which assumes a constant slope within the footprint, or the point-based method, which assumes a fixed footprint size ~~and defines the reflecting point as the shortest mean range of points within each assumed footprint~~to determine the impact point by minimising the mean distance. Each of these methods has ~~shortcoming~~ shortcomings as they either neglect the actual topography or the actual footprint that can be estimated by a combination of the leading edge and topography.

~~To overcome this shortcoming~~To overcome these shortcomings, we present a ~~novel~~ Leading Edge Point-Based (LEPTA) method that corrects for the slope-induced error by including the leading edge information of the radar waveform to determine the impact point. The principle of the method is that only the points on the ground that are within range determined by ~~the begin and end of the~~ a specific search range that contributes to the rise of the waveform leading edge are used to determine the impact point. ~~This requires the assistance of a high-resolution DEM, e. g. 100 m resolution.~~

Different methods for correcting the slope-induced errors are used in this study using CryoSat-2 measurements over the Greenland ice sheet. Statistics show that the LEPTA method outperforms all other methods with the smallest median and variability of errors. The median ~~is almost identical to the~~ difference between ICESat-2 ~~height measurements~~heights and CryoSat-2 heights derived by LEPTA using a 20% OCOG threshold and $\Delta r = 1.25$ m search range is 0.00 m. Spatially, LEPTA has a good improvement compared to the traditional slope method on the margins of the ~~ice sheet.~~ LRM-covered regions of the ice sheet, as it derives heights generally more than 2 m closer to ICESat-2 measurements. LEPTA is sensitive to the definition of the search range, and the bias in the DEM used to correct for the slope-induced error, mainly in the horizontal location of the impact points. However, comparison with ICESat-2 measurements generally shows centimetre-level sensitivity. Therefore, LEPTA is a method worth considering to obtain accurate height measurements with radar ~~altimeter~~altimetry, especially in regions with complex topography.

Appendix A: Comparison between ICESat-2 measurements and ArcticDEM

ICESat-2 ALT06 Land Ice Height data include a large amount of measurements between Jan. 1 and Dec. 31 2019. Therefore, we compute the statistics of the differences between ICESat-2 heights (h_{ICE2}) and ArcticDEM interpolated to the corresponding locations (h_{DEMI}) per beam pair. The statistics are summarised in Table A1. All differences are computed as $h_{\text{ICE2}} - h_{\text{DEMI}}$. The median difference between ICESat-2 and ArcticDEM is for all beam pairs < 0.02 m, showing good agreement. The mean differences are around 3.70 m.

Appendix B: Full probability distribution functions of the height differences

Full probability distribution functions of all methods are provided in Figs. B1-B1 to illustrate the underlying skewness in Table 1 and Fig. 3-Fig. 4. For the slope method, the DEM resolution is 2 km. For LEPTA, the Δr is 1.25 m. For the slope method, point-based method and LEPTA, the retracker is the OCOG retracker with a 20% threshold.

Appendix C: Impact of a bias in the ArcticDEM on the 3D location of the LEPTA impact points

Figures C1- C2 show the three-dimensional difference between using the original ArcticDEM and the vertically displaced DEM to correct for the slope-induced error. The vertical and horizontal differences are calculated using the difference between the location of impact points P_l of the biased DEM minus the location of the impact points of the original ArcticDEM. Figure C1 shows that when the DEM used has a negative bias, the corrected heights are higher, the horizontal locations on the western side of the ice sheet are in general biased towards the northeast, and the horizontal locations on the northeast side of the ice sheet are biased towards the southwest. Figure C2 shows an inverse pattern, when the DEM shows a positive bias. On the interior of the ice sheet, however, the effects of the DEM biases are small.

Author contributions. WL conducted data management, processing and analysis, produced the figures, and provided the manuscript with contributions from all co-authors. CS designed the study and provided expertise and software for radar-altimetry processing. SL provided support on statistical analysis and data visualisation.

Competing interests. The authors declare they have no conflict of interest.

Acknowledgements. The research is supported by the Dutch Research Council (NWO) on the ALWGO.2017.033 project.

ArcticDEM is provided by the Polar Geospatial Center under NSF-OPP awards 1043681, 1559691, and 1542736. DEM of Greenland used for result visualisation is provided by Helm et al. (2014a, b) under license Creative Commons Attribution 3.0 Unported. The CryoSat-2 L1b and L2I data are provided online by ESA and the ICESat-2 L3A data are provided online by NSIDC (https://nsidc.org/data/atl06).

The authors would also like to thank Professor Roland Klees, Dr Bert Wouters, Katarzyna Sejan, Jan Haacker and Dr Lorenzo Iannini for valuable discussions, and Dr Louise Sandberg Sørensen for the review and editing of this ~~draft~~manuscript. Finally, we would like to thank the referees for reviewing and providing recommendations to improve this manuscript.

References

Abdalati, W., Zwally, H. J., Bindschadler, R., Csatho, B., Farrell, S. L., Fricker, H. A., Harding, D., Kwok, R., Lefsky, M., Markus, T., et al.: The ICESat-2 laser altimetry mission, Proceedings of the IEEE, 98, 735–751, 2010.

Adodo, F. I., Remy, F., and Picard, G.: Seasonal variations of the backscattering coefficient measured by radar altimeters over the Antarctic Ice Sheet, The Cryosphere, 12, 1767–1778, https://doi.org/10.5194/tc-12-1767-2018, 2018.

Aublanc, J., Moreau, T., Thibaut, P., Boy, F., Rémy, F., and Picot, N.: Evaluation of SAR altimetry over the antarctic ice sheet from CryoSat-2 acquisitions, Advances in Space Research, 62, 1307–1323, https://doi.org/10.1016/j.asr.2018.06.043, 2018.

Bamber, J. L.: Ice sheet altimeter processing scheme, International Journal of Remote Sensing, 15, 925–938, https://doi.org/10.1080/01431169408954125, 1994.

Blarel, F. and Legresy, B.: Investigations on the Envisat RA2 Doppler slope correction for ice sheets, in: European Space Agency-CNES Symp., Venice, Italy, 2012.

Bobach, T. A.: Natural Neighbor Interpolation - Critical Assessment and New Contributions, Ph.D. thesis, Technische Universität Kaiserslautern, 2009.

Bouzinac, C.: CryoSat Product Handbook, Tech. rep., ESA, https://earth.esa.int/documents/10174/125272/CryoSat_Product_Handbook, 2012.

Brenner, A. C., Bindschadler, R. A., Thomas, R. H., and Zwally, H. J.: Slope-induced errors in radar altimetry over continental ice sheets, Journal of Geophysical Research, 88, 1617, https://doi.org/10.1029/jc088ic03p01617, 1983.

Brenner, A. C., DiMarzio, J. P., and Zwally, H. J.: Precision and Accuracy of Satellite Radar and Laser Altimeter Data Over the Continental Ice Sheets, IEEE Transactions on Geoscience and Remote Sensing, 45, 321–331, https://doi.org/10.1109/tgrs.2006.887172, 2007.

Cooper, A.: Slope Correction By Relocation For Satellite Radar Altimetry, in: 12th Canadian Symposium on Remote Sensing Geoscience and Remote Sensing Symposium, IEEE, https://doi.org/10.1109/igarss.1989.577978, 1989.

Davis, C.: A robust threshold retracking algorithm for measuring ice-sheet surface elevation change from satellite radar altimeters, IEEE Transactions on Geoscience and Remote Sensing, 35, 974–979, https://doi.org/10.1109/36.602540, 1997.

European Space Agency: L1b LRM Precise Orbit. Baseline D, https://doi.org/10.5270/CR2-cbow23i, 2019a.

European Space Agency: L2 LRM Precise Orbit. Baseline D, https://doi.org/10.5270/CR2-k1o4pyh, 2019b.

Hai, G., Xie, H., Du, W., Xia, M., Tong, X., and Li, R.: Characterizing slope correction methods applied to satellite radar altimetry data: A case study around Dome Argus in East Antarctica, Advances in Space Research, 67, 2120–2139, https://doi.org/10.1016/j.asr.2021.01.016, 2021.

Helm, V., Humbert, A., and Miller, H.: Elevation and elevation change of Greenland and Antarctica derived from CryoSat-2, The Cryosphere, 8, 1539–1559, https://doi.org/10.5194/tc-8-1539-2014, 2014a.

Helm, V., Humbert, A., and Miller, H.: Elevation Model of Greenland derived from CryoSat-2 in the period 2011 to 2013, links to DEM and uncertainty map as GeoTIFF, https://doi.org/10.1594/PANGAEA.831393, 2014b.

Howat, I. M., Porter, C., Smith, B. E., Noh, M.-J., and Morin, P.: The Reference Elevation Model of Antarctica, The Cryosphere, 13, 665–674, https://doi.org/10.5194/tc-13-665-2019, 2019.

Hurkmans, R. T. W. L., Bamber, J. L., and Griggs, J. A.: Brief communication "Importance of slope-induced error correction in volume change estimates from radar altimetry", The Cryosphere, 6, 447–451, https://doi.org/10.5194/tc-6-447-2012, 2012.

Lacroix, P., Dechambre, M., Legrésy, B., Blarel, F., and Rémy, F.: On the use of the dual-frequency ENVISAT altimeter to determine snowpack properties of the Antarctic ice sheet, Remote Sensing of Environment, 112, 1712–1729, https://doi.org/10.1016/j.rse.2007.08.022, 2008.

Levinsen, J. F., Simonsen, S. B., Sorensen, L. S., and Forsberg, R.: The Impact of DEM Resolution on Relocating Radar Altimetry Data Over Ice Sheets, IEEE Journal of Selected Topics in Applied Earth Observations and Remote Sensing, 9, 3158–3163, https://doi.org/10.1109/jstars.2016.2587684, 2016.

Meloni, M., Bouffard, J., Parrinello, T., Dawson, G., Garnier, F., Helm, V., Bella, A. D., Hendricks, S., Ricker, R., Webb, E., Wright, B., Nielsen, K., Lee, S., Passaro, M., Scagliola, M., Simonsen, S. B., Sørensen, L. S., Brockley, D., Baker, S., Fleury, S., Bamber, J., Maestri, L., Skourup, H., Forsberg, R., and Mizzi, L.: CryoSat Ice Baseline-D validation and evolutions, The Cryosphere, 14, 1889–1907, https://doi.org/10.5194/tc-14-1889-2020, 2020.

Noh, M.-J. and Howat, I. M.: Automated stereo-photogrammetric DEM generation at high latitudes: Surface Extraction with TIN-based Search-space Minimization (SETSM) validation and demonstration over glaciated regions, GIScience & Remote Sensing, 52, 198–217, https://doi.org/10.1080/15481603.2015.1008621, 2015.

Noh, M.-J. and Howat, I. M.: The Surface Extraction from TIN based Search-space Minimization (SETSM) algorithm, ISPRS Journal of Photogrammetry and Remote Sensing, 129, 55–76, https://doi.org/10.1016/j.isprsjprs.2017.04.019, 2017.

Porter, C., Morin, P., Howat, I., Noh, M.-J., Bates, B., Peterman, K., Keesey, S., Schlenk, M., Gardiner, J., Tomko, K., Willis, M., Kelleher, C., Cloutier, M., Husby, E., Foga, S., Nakamura, H., Platson, M., Wethington, Michael, J., Williamson, C., Bauer, G., Enos, J., Arnold, G., Kramer, W., Becker, P., Doshi, A., D'Souza, C., Cummens, P., Laurier, F., and Bojesen, M.: ArcticDEM, https://doi.org/10.7910/DVN/OHHUKH, 2018.

Remy, F., Mazzega, P., Houry, S., Brossier, C., and Minster, J.: Mapping of the Topography of Continental Ice by Inversion of Satellite-altimeter Data, Journal of Glaciology, 35, 98–107, https://doi.org/10.3189/002214389793701419, 1989.

Roemer, S., Legrésy, B., Horwath, M., and Dietrich, R.: Refined analysis of radar altimetry data applied to the region of the subglacial Lake Vostok/Antarctica, Remote Sensing of Environment, 106, 269–284, https://doi.org/10.1016/j.rse.2006.02.026, 2007.

Schröder, L., Horwath, M., Dietrich, R., Helm, V., van den Broeke, M. R., and Ligtenberg, S. R. M.: Four decades of Antarctic surface elevation changes from multi-mission satellite altimetry, The Cryosphere, 13, 427–449, https://doi.org/10.5194/tc-13-427-2019, 2019.

Simonsen, S. B. and Sørensen, L. S.: Implications of changing scattering properties on Greenland ice sheet volume change from Cryosat-2 altimetry, Remote Sensing of Environment, 190, 207–216, https://doi.org/10.1016/j.rse.2016.12.012, 2017.

Slater, T., Shepherd, A., McMillan, M., Muir, A., Gilbert, L., Hogg, A. E., Konrad, H., and Parrinello, T.: A new digital elevation model of Antarctica derived from CryoSat-2 altimetry, The Cryosphere, 12, 1551–1562, https://doi.org/10.5194/tc-12-1551-2018, 2018.

Smith, B., Fricker, H. A., Holschuh, N., Gardner, A. S., Adusumilli, S., Brunt, K. M., Csatho, B., Harbeck, K., Huth, A., Neumann, T., Nilsson, J., and Siegfried, M. R.: Land ice height-retrieval algorithm for NASA's ICESat-2 photon-counting laser altimeter, Remote Sensing of Environment, 233, 111 352, https://doi.org/10.1016/j.rse.2019.111352, 2019.

Smith, B., Fricker, H. A., Gardner, A., Siegfried, M. R., Adusumilli, S., Csathó, B. M., Holschuh, N., Nilsson, J., Paolo, F. S., and the ICESat-2 Science Team: ATLAS/ICESat-2 L3A Land Ice Height, Version 4, https://doi.org/10.5067/ATLAS/ATL06.004, [Date Accessed 2020-09-01], 2020a.

Smith, B., Hancock, D., Harbeck, K., Roberts, L., Neumann, T., Brunt, K., Fricker, H., Gardner, A., Siegfried, M., Adusumilli, S., Csathó, B., Holschuh, N., Nilsson, J., and Paolo, F.: Algorithm Theoretical Basis Document (ATBD) for Land Ice Along-Track Height Product

(ATL06), Tech. rep., ICESat-2 Project Science Office, https://nsidc.org/sites/nsidc.org/files/technical-references/ICESat2_ATL06_ATBD_r004.pdf, 2020b.

Wingham, D., Rapley, C., and D, G.: New Techniques in Satellite Altimeter Tracking Systems, in: Digest - International Geoscience and Remote Sensing Symposium (IGARSS), vol. ESA SP-254, pp. 1339–1344, Zurich, 1986.

Table 1. Statistics of the height difference between slope-corrected CryoSat-2 measurements and ArcticDEM and ICESat-2 ($h_C - h_{\mathrm{DEMC}}$ or Δh as computed by Eq. (16)). Height statistics are in unit of metres. ~~Before and after in the table represent the~~ The parameters ~~before~~ are shown with and ~~after removing~~ without outliers (referred to as w/ outlier and w/o outlier) using 10th and 90th percentiles. E, S, P and L represent ESA L2I, slope method, point-based method and LEPTA, respectively.

CryoSat-2		vs. ArcticDEM E	S	P	L	vs. ICESat-2 E	S	P	L
No. of data	w/ outlier	~~2.4~~2.2e6	2.2e6	2.2e6	2.2e6	~~9.1~~8.2e4	8.3e4	8.3e4	8.2e4
	w/o outlier	~~2.0~~1.8e6	1.8e6	1.8e6	1.8e6	~~7.3~~6.6e4	6.6e4	6.6e4	6.6e4
median	w/ outlier	~~-41.7~~ 0.43	~~-1.18~~ 0.69	~~-4.37~~ 0.71	~~-2.43~~ 0.24	~~-39.7~~ 0.01	~~-0.51~~ 0.21	~~-2.15~~ 0.48	~~-1.12~~ 0.00
	w/o outlier	~~-0.85~~ 0.43	~~-0.17~~ 0.69	~~0.03~~ 0.71	~~-0.60~~ 0.24	~~-0.37~~ 0.01	~~-0.08~~ 0.21	~~0.42~~ 0.48	~~-0.25~~ 0.00
median absolute deviation	w/ outlier	~~-3.13~~ 0.58	~~-0.48~~ 0.66	~~-0.52~~ 0.45	~~-1.03~~ 0.45	~~-2.00~~ 0.18	~~-0.17~~ 0.24	~~0.28~~ 0.14	~~-0.42~~ 0.12
	w/o outlier	~~-0.61~~ 0.44	~~-0.06~~ 0.50	~~0.18~~ 0.35	~~-0.46~~ 0.34	~~-0.28~~ 0.14	~~-0.05~~ 0.19	~~0.46~~ 0.10	~~-0.20~~ 0.09
mean	w/ outlier	~~-0.94~~ 0.58	~~-0.20~~ 1.27	~~-0.01~~ 0.47	~~-0.64~~ 0.22	~~-0.40~~ 0.39	~~-0.09~~ 1.14	~~0.40~~ 0.39	~~-0.26~~ ~~w/o outlier~~ ~~-0.42~~ 0.06 ~~0.32~~ ~~-0.34~~ ~~-0.22~~ ~~-0.02~~ ~~0.49~~ ~~-0.16~~
	w/~~outlier~~ ~~2.02 5.12~~ ~~1.90 1.22~~ ~~1.62 4.80~~ ~~1.31 0.44~~ ~~w/~~o outlier	~~1.27~~ 0.51	~~2.65~~ 0.87	~~1.58~~ 0.70	~~0.88~~ 0.22	~~0.68~~ 0.13	~~2.21~~ 0.51	~~1.06~~ 0.50	~~0.20~~ 0.00
standard deviation	w/ outlier	~~3.38~~ 2.87	~~9.23~~ 3.11	~~2.25~~ 2.75	~~1.75~~ ~~3.41~~ ~~9.09~~	~~1.02~~ 2.73	~~1.01~~ 3.27	~~3.20~~ 1.78	~~1.17~~ ~~0.27~~ 1.64

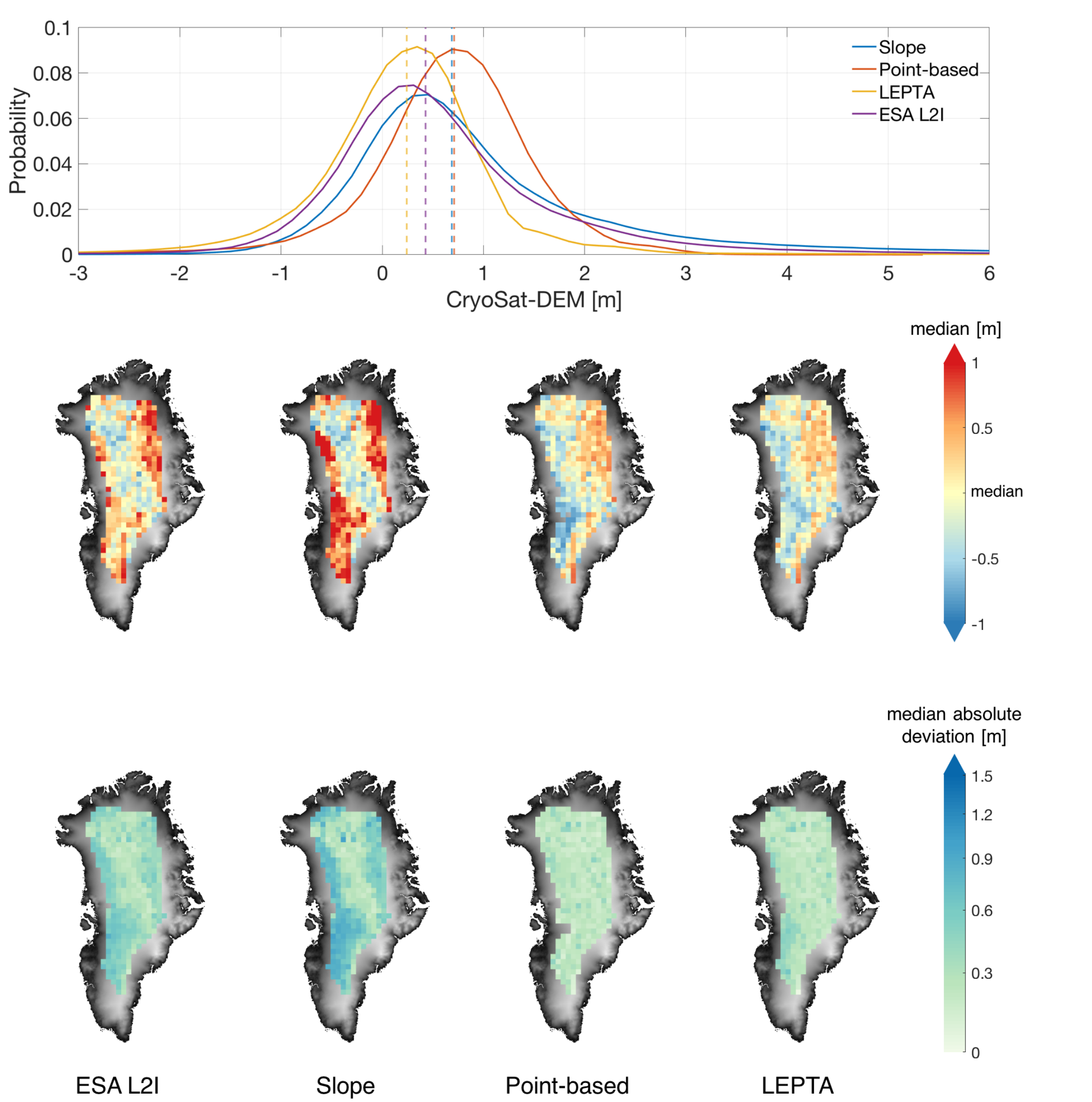

Figure 3. Upper panel: probability distribution of height difference between CryoSat-2 and the ArcticDEM, before removing the outliers with 10th and 90th percentiles. The probability distribution is plotted with all data samples, but restricted to [-3m, 6m] for visualisation (for full distribution please refer to Appendix B). Vertical lines show median value per method. Middle and ~~medium and~~ lower ~~panel~~panels: spatial distribution of median and median absolute deviation of the height difference per tile of ~~50~~ 50×50 km~~$\times$ 50 km~~, after removing the outliers. ~~The probability distribution is plotted with all data samples~~To enhance the visibility of the maps, ~~but restricted to -3m, 6mfor visualisation~~the median value of each method is subtracted in the middle panel. The colours of the gridded plots are in logarithmic scale to enhance contrast. The spatial distribution results from left to right are obtained by ESA L2I products, the slope method, the point-based method and LEPTA, with the ~~1~~ 1×1 km ~~$\times$ 1 km~~ DEM covering Greenland (Helm et al., 2014a, b) as background.

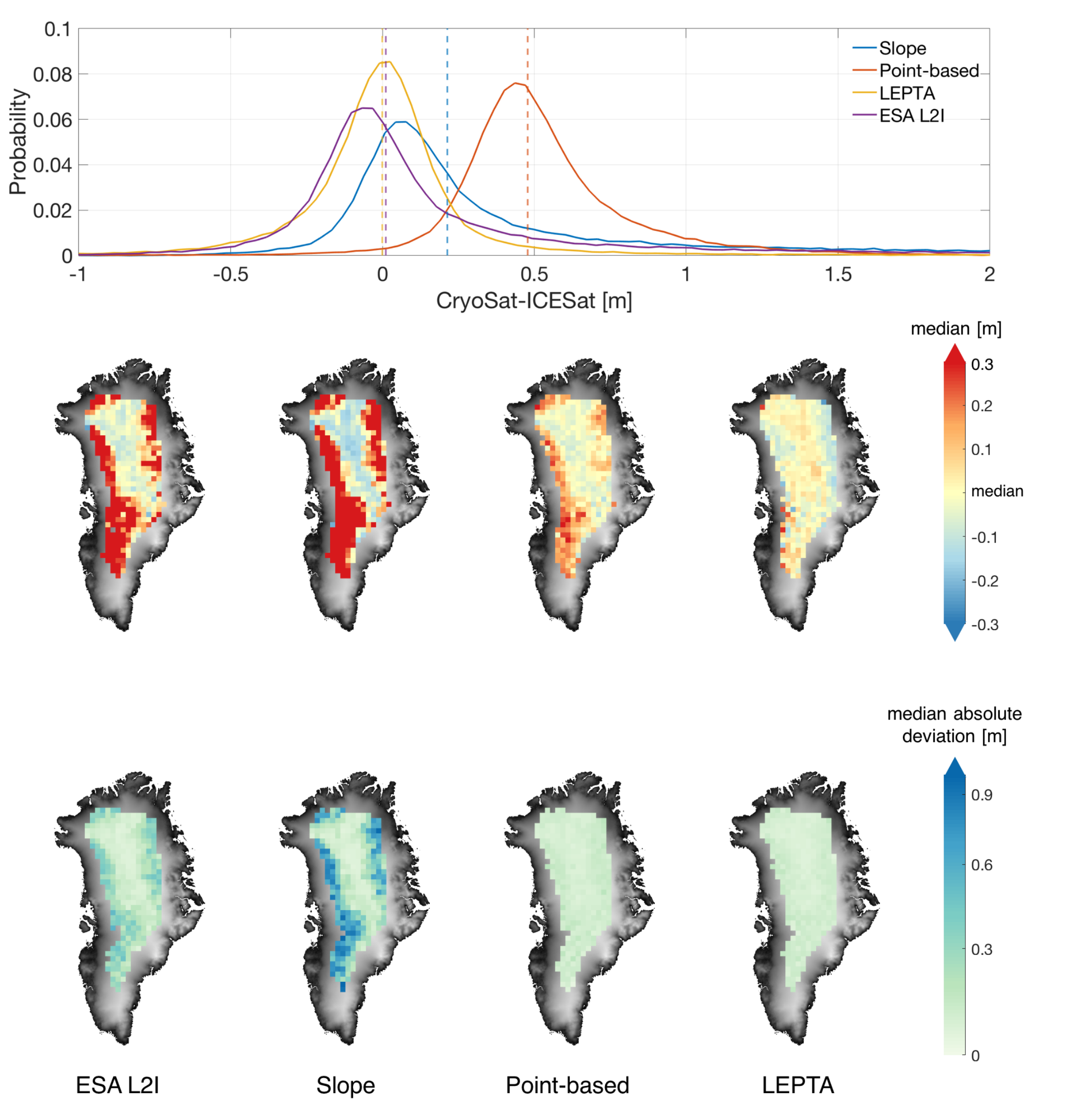

Figure 4. Upper panel: probability distribution of height difference between CryoSat-2 and the ICESat-2, before removing the outliers. The probability distribution is plotted with all data samples, but restricted to [-1 m, 2 m] for visualisation (for the full distribution we refer to Appendix B). Vertical lines show median value per method. Middle and ~~medium and~~ lower ~~panel~~panels: spatial distribution of median and median absolute deviation of the height difference per tile of 50 km × 50 km, after removing the outliers. ~~The probability distribution~~ To enhance the visibility of the maps the median value of each method is ~~plotted with all data samples, but restricted to -1 m, 2 mfor visualisation~~subtracted in the middle panel. The colours of the gridded plots are in logarithmic scale. The spatial distribution results from left to right are obtained by ESA L2I products, the slope method, the point-based method and LEPTA, with the ~~1~~ 1 × 1 km ~~× 1 km~~ DEM covering Greenland (Helm et al., 2014a, b) as background.

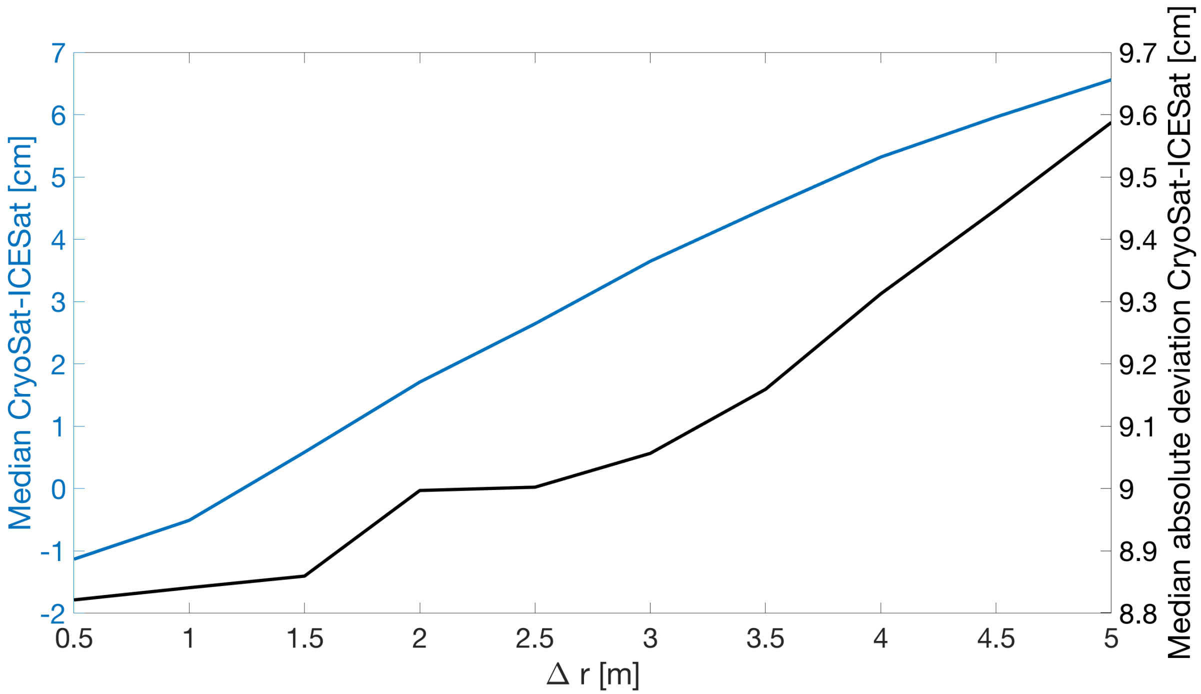

Figure 5. Median (left axis) and median absolute deviation (right axis) of the height differences between CryoSat-2 and ICESat-2 (Δh calculated with Eq. (16)) as function of Δr. As Δr increases, the former curve varies within millimetre level, Outliers are removed using 10th and the latter varies within centimetre level90th percentiles.

Table A1. Difference between ICESat-2 measurements and ArcticDEM values interpolated to ICESat-2 locations.

Beam pair of measurements	vs. ArcticDEM [m]			
	mean	standard deviation	median	median absolute deviation
pair one	3.70	48.01	0.01	0.81
pair two	3.72	48.30	0.01	0.81
pair three	3.68	48.10	0.02	0.81

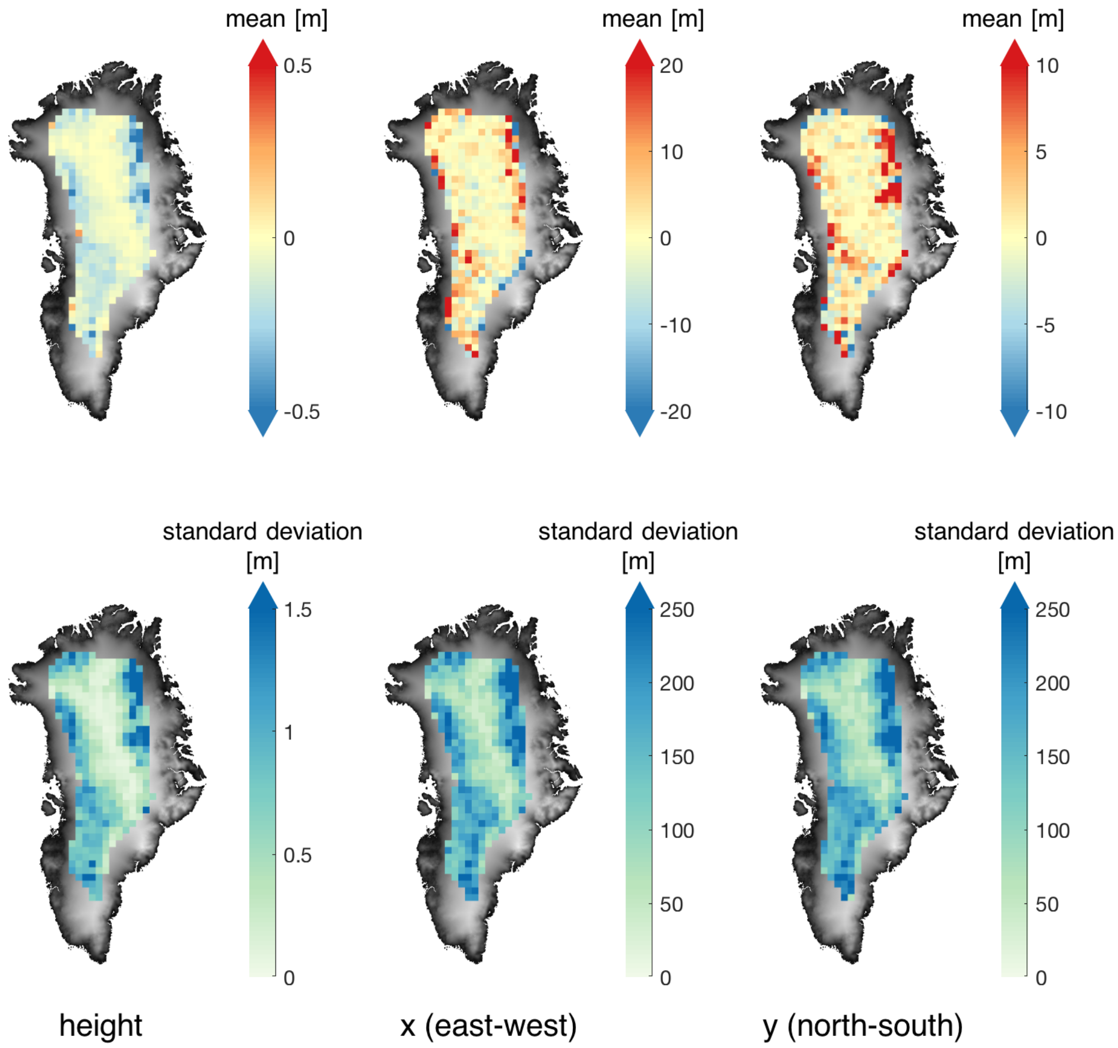

Figure 6. Mean and standard deviation of the differences between the height and horizontal location of the impact point obtained using $\Delta r = 2$ m (Δr_2) and $\Delta r = 1$ m (Δr_1). The mapped locations are based on the horizontal locations (x and y) derived from Δr_1, tiled by the 50×50 km grid same as in Fig. 4.

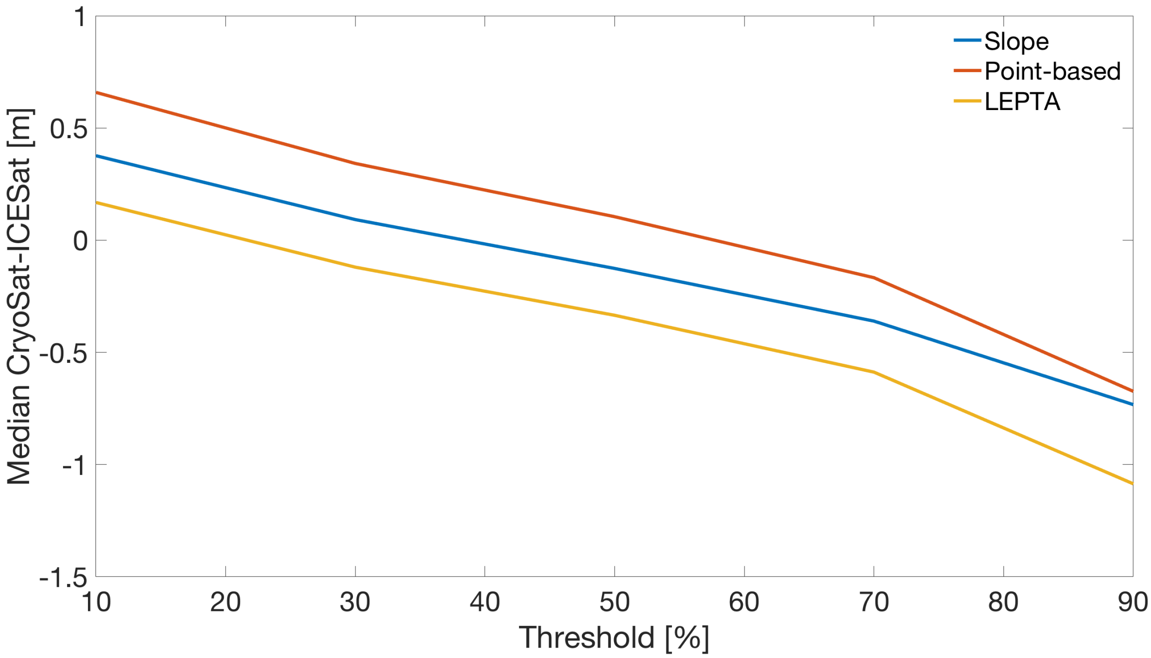

Figure 7. Median of height differences between CryoSat-2 and ICESat-2 (Δh calculated with Eq. (16)) as function of the OCOG retracker threshold. Outliers are removed using 10th and 90th percentiles.

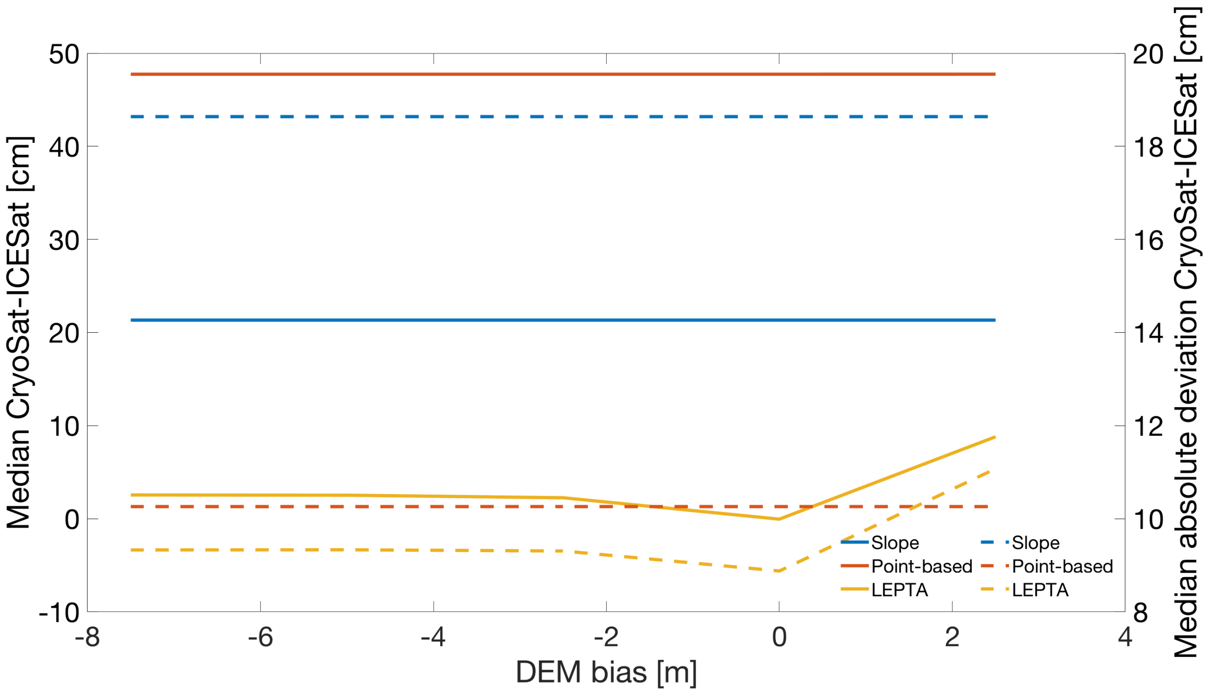

Figure 8. Median (left axis, solid curves) and median absolute deviation (right axis, dashed curves) of height differences between CryoSat-2 and ICESat-2 (Δh calculated with Eq. (16)) as function of a bias in the DEM. ~~LEPTA performs best with the original DEM~~Outliers are removed using 10th and 90th percentiles.

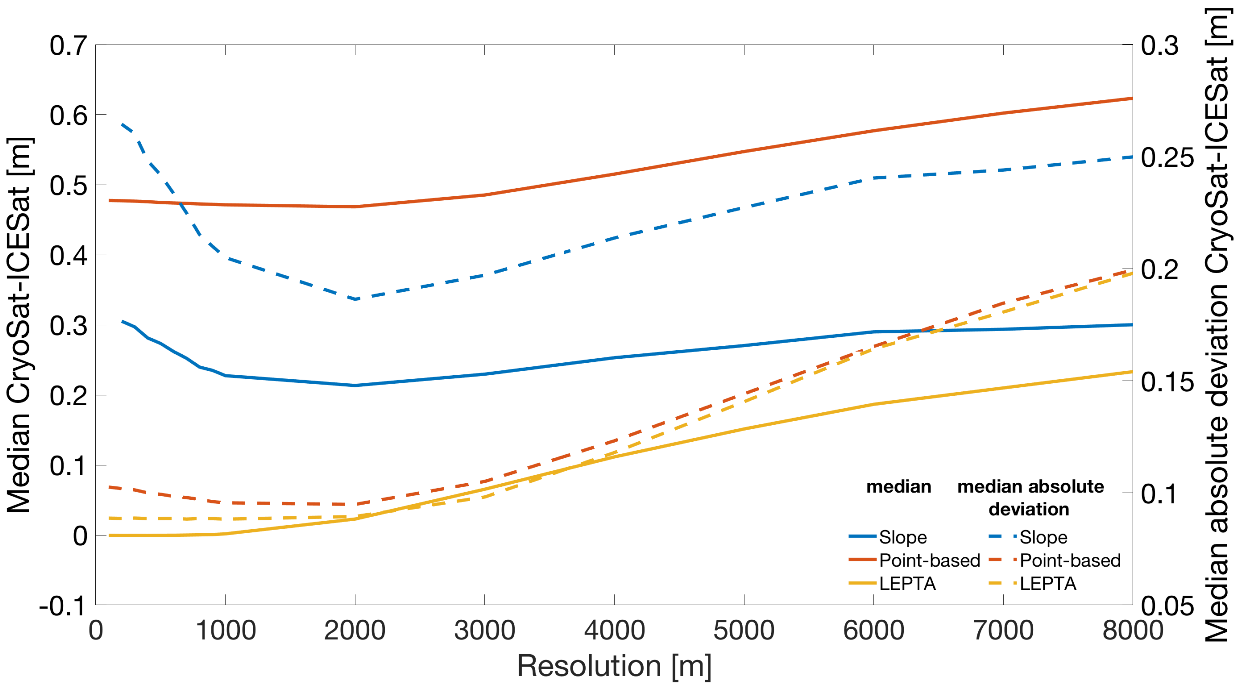

Figure 9. Median (left axis, solid curves) and median absolute deviation (right axis, dashed curves) of height differences between CryoSat-2 and ICESat-2 (Δh calculated with Eq. (16)) as a function of DEM resolution. ~~Both the point-based method~~ Outliers are removed using 10th and ~~LEPTA have a decreasing accuracy with decreasing DEM resolution, while the slope method has an increasing accuracy with an decreasing DEM resolution~~90th percentiles.

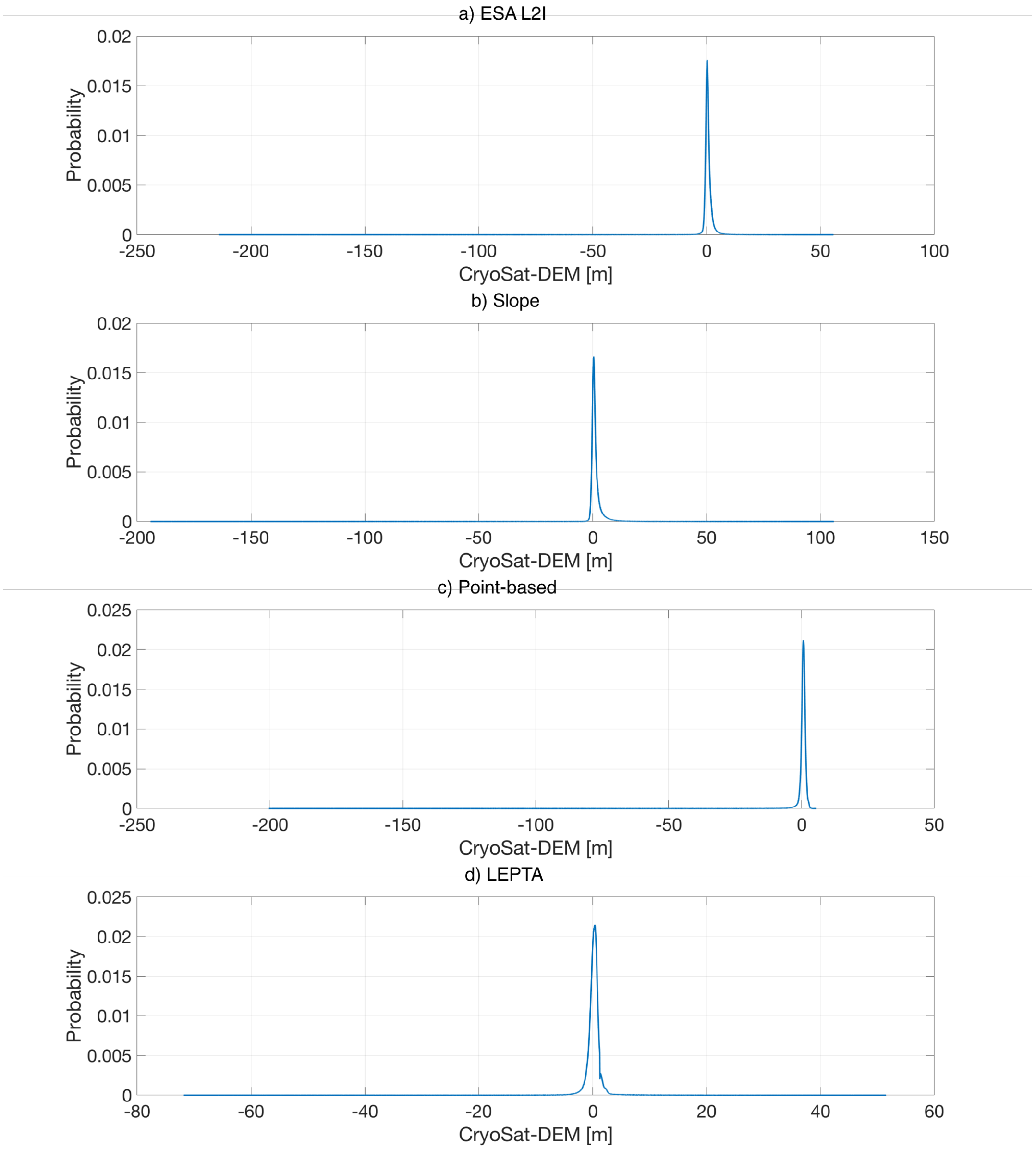

Figure B1. Full probability distribution functions of heights between CryoSat-2 and ArcticDEM derived from a) ESA L2I, b) slope method, c) point-based method and d) LEPTA.

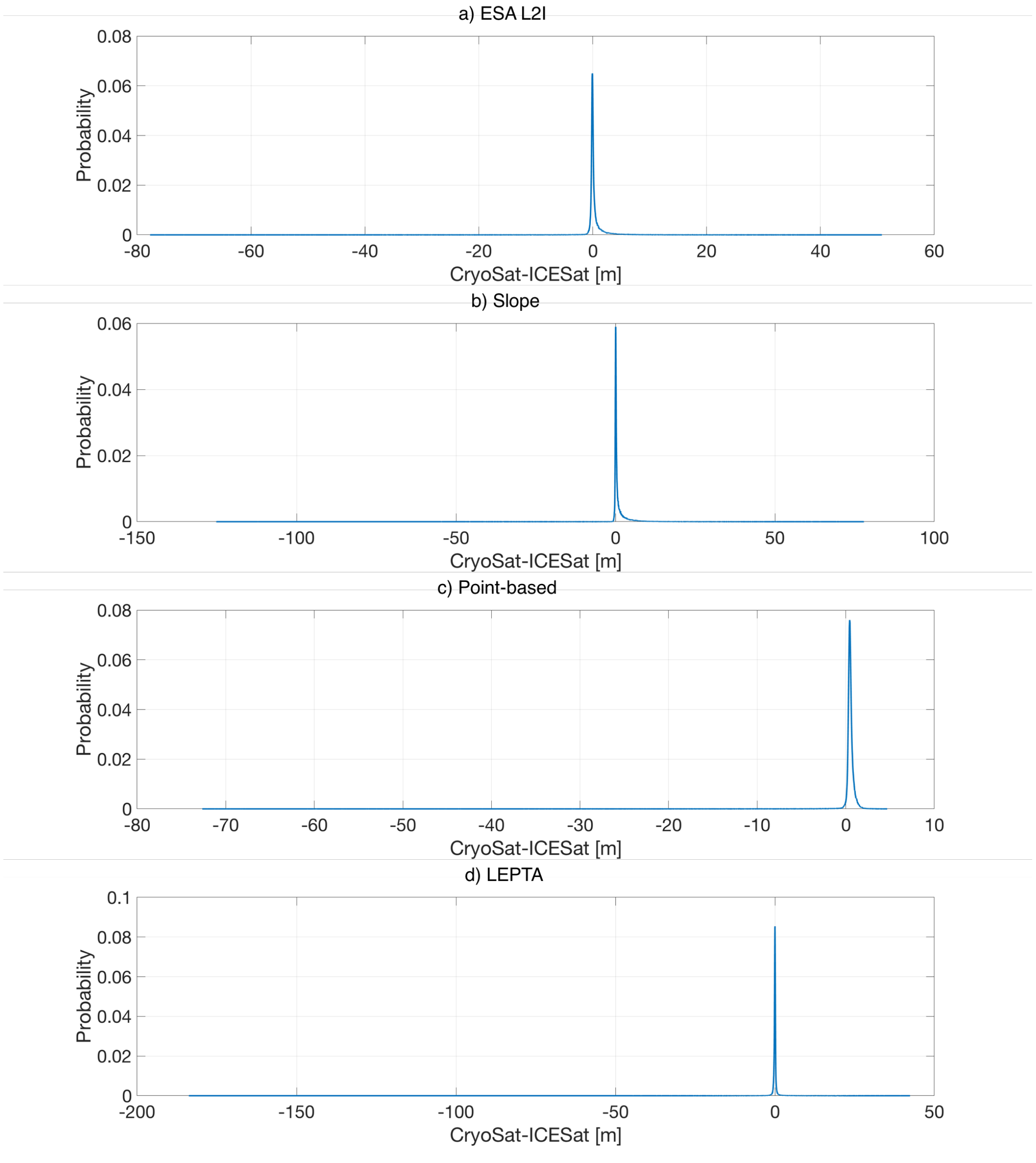

Figure B2. Full probability distribution functions of heights between CryoSat-2 and ICESat-2 derived from a) ESA L2I, b) slope method, c) point-based method and d) LEPTA.

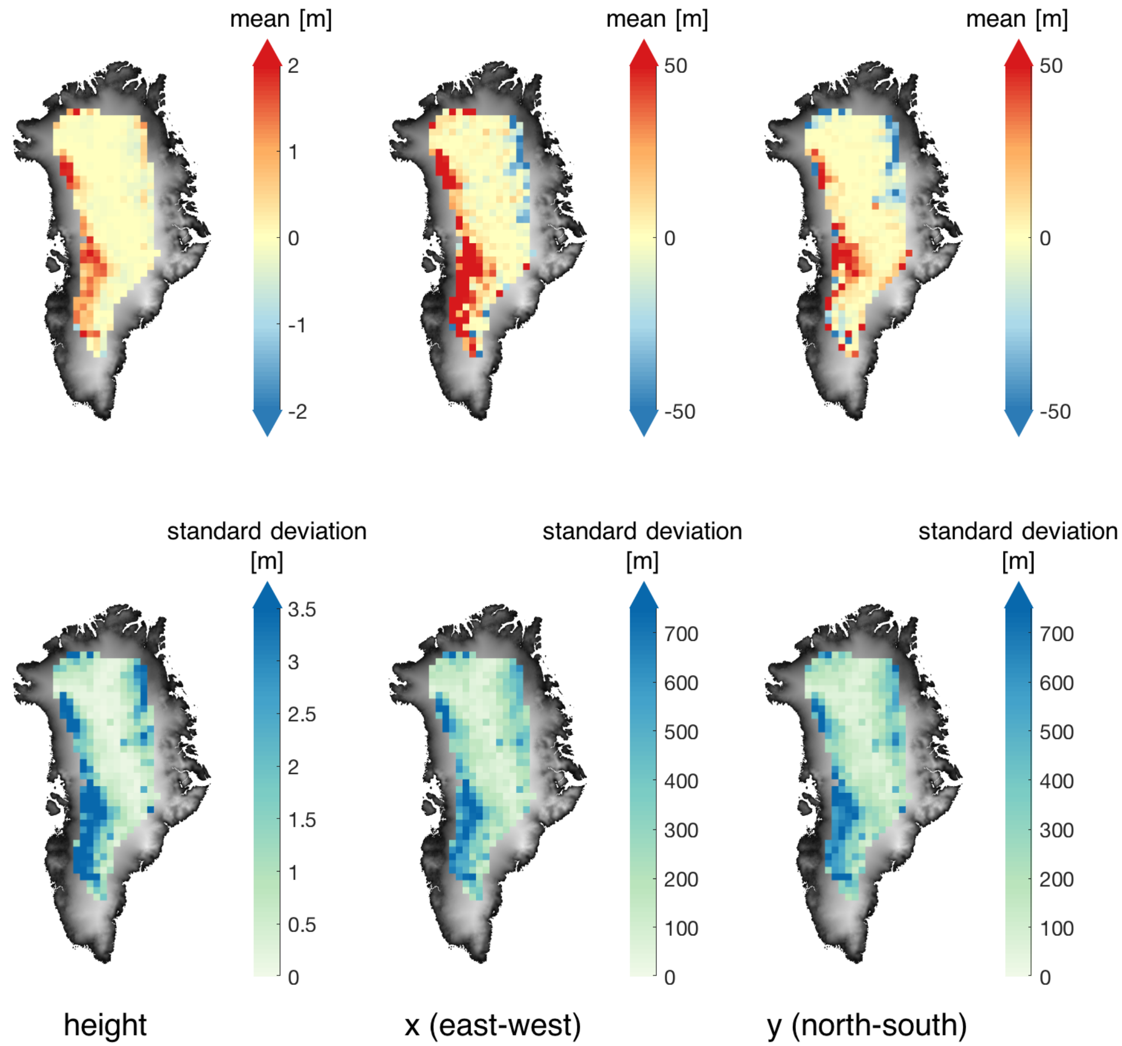

Figure C1. Mean and standard deviation of vertical and horizontal difference of derived impact point P_l between i) using the DEM with a homogeneous vertical displacement $\Delta h_{\mathrm{DEM}} = -2.5$ m (Δh_{DEM1}) and ii) using the original ArcticDEM ($\mathrm{DEM}_{\mathrm{orig}}$). The mapped locations are based on the horizontal locations (x and y) derived from $\mathrm{DEM}_{\mathrm{orig}}$, tiled by the 50×50 km grid same as in Fig. 6.

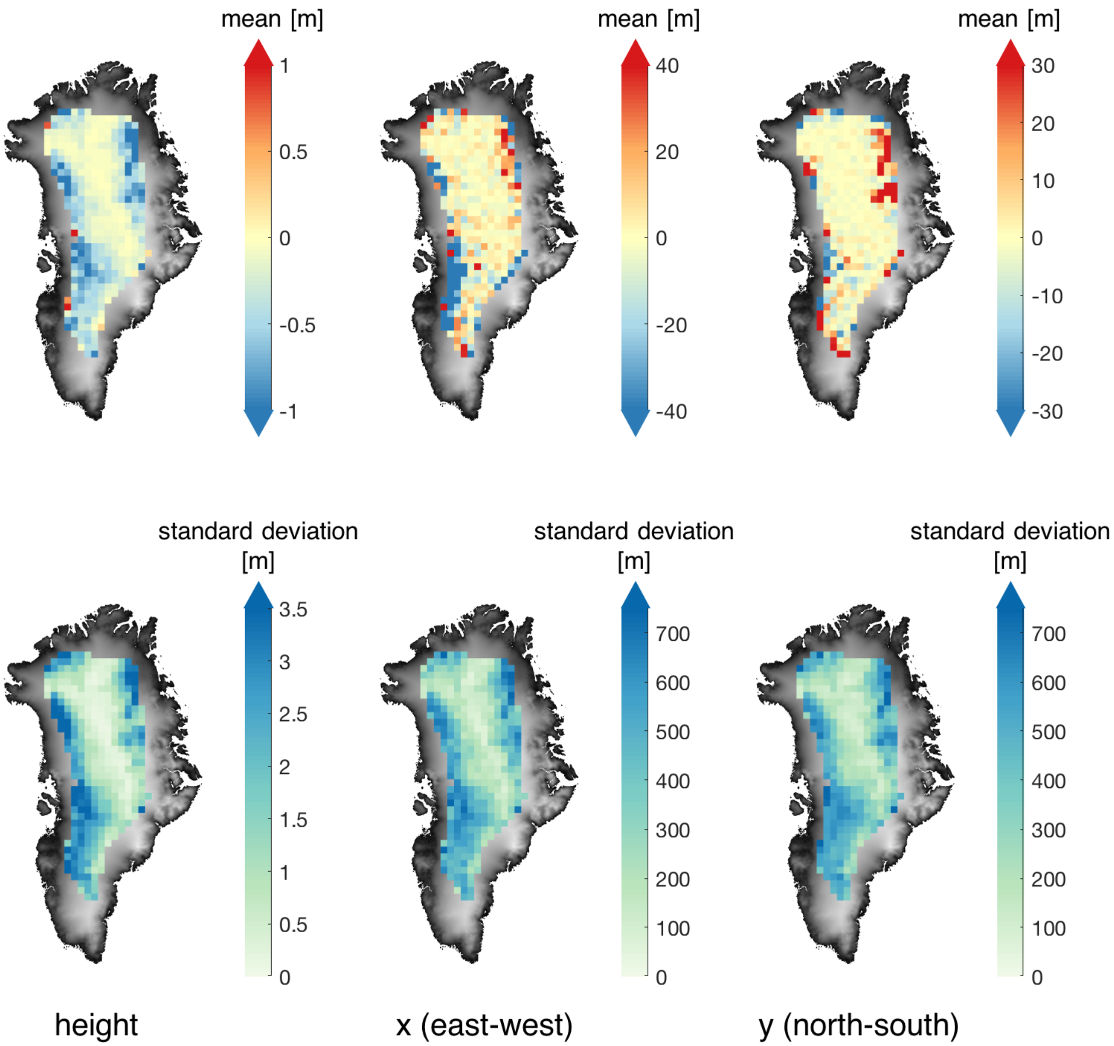

Figure C2. Mean and standard deviation of vertical and horizontal difference of derived impact point P_I between i) using the DEM with a homogeneous vertical displacement $\Delta h_{\mathrm{DEM}} = 2.5$ m (Δh_{DEM1}) and ii) using the original ArcticDEM ($\mathrm{DEM_{orig}}$). The mapped locations are based on the horizontal locations (x and y) derived from $\mathrm{DEM_{orig}}$, tiled by the 50×50 km grid same as in Fig. 6.